

Fig. 2. Notch was endocytosed but not transported to early endosomes in *O-fut1*⁻ cells. (A-K) Live wing discs containing *Notch*⁻ (A,B) or *O-fut1*⁻ (C-K) clones were incubated with an anti-Notch extracellular antibody (rat1; magenta) to detect Notch on the plasma membrane, and allowed to endocytose Notch for 20 minutes (A-J) or 10 hours (K). Mutant cells were distinguished by the lack of GFP (green, A-F,K) or are labeled *O-fut1*⁻ (G-J). Wing discs were also stained with an anti-Hrs antibody (G-J, shown in green). Optical sections corresponding to the apical region (A,C,G) or to 2 μ m (D,H) or 8 μ m (E,I) beneath the apical level, and optical vertical sections (B,F,J) are shown. (L) Living wing discs with *O-fut1*⁻ clones (indicated by *O-fut1*⁻) incubated with fluorescent dextran (green) for 10 minutes, chased for 20 minutes at 25°C, and stained with an anti-Notch antibody (C17.9C6; magenta). Higher magnification of one or two dextran-positive vesicles in wild-type (arrowhead) and *O-fut1*⁻ (open arrowhead) cells are shown as insets in the upper left and lower right, respectively. The clone boundaries are demarcated by a white dashed line. All wing discs were isolated from late third-instar larvae.

standard confocal microscope, Notch appeared to mostly co-localize with PDI-GFP in *O-fut1*⁻ cells, which was consistent with the previous report (Okajima et al., 2005) (Fig. 3A). However, higher resolution images obtained by deconvolution analysis revealed that this ER marker did not co-localize with the Notch-containing vesicles in *O-fut1*⁻ cells (Fig. 3B,C). Similar results were obtained using ER-CFP as the ER marker (Fig. 3D,E). In the positive control,

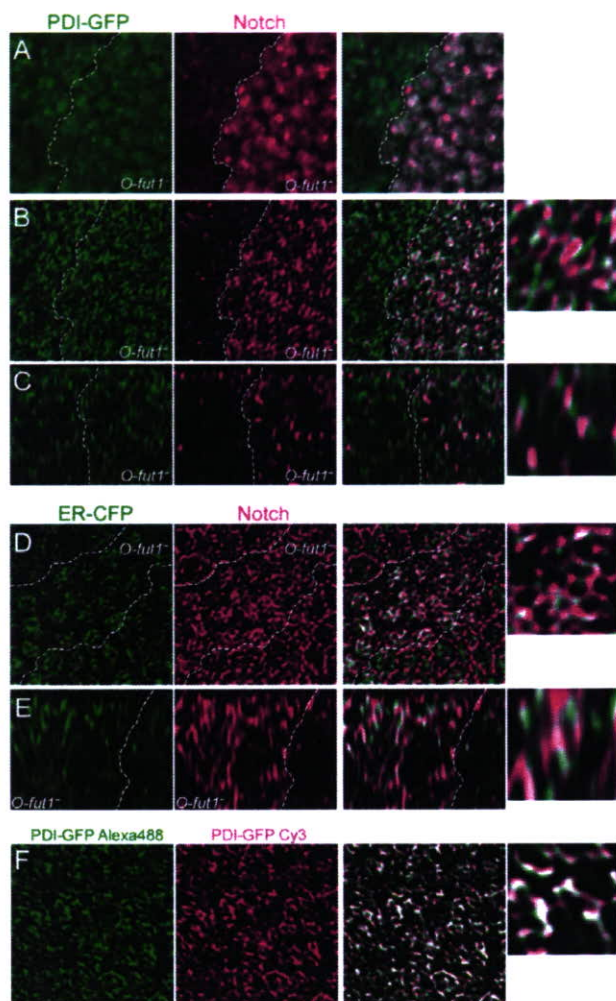


Fig. 3. Most Notch was not co-localized with ER markers in *O-fut1*⁻ cells. (A-E) *O-fut1*⁻ somatic clones (labeled *O-fut1*⁻) generated in wing discs expressing ER marker PDI-GFP (A-C) or ER-CFP (driven by *sd-GAL4*; D,E), and stained with anti-Notch (C17.9C6, magenta) and anti-GFP (green) antibodies. (A) Normal confocal image showing the subapical region of the wing disc epithelium, where Notch accumulated in *O-fut1*⁻ cells. (B) The resolution of A was improved using deconvolution. (C) Optical vertical section of B. (D) Deconvolution was used to improve the resolution of this image. (E) Optical vertical section of D. (F) A positive control for deconvolution analysis. Wing discs expressing PDI-GFP were incubated with a rat anti-GFP antibody, and stained simultaneously with two anti-rat secondary antibodies, conjugated to Alexa 488 or Cy3. All wing discs were isolated from late third-instar larvae. Right panels show merged images of the left and middle panels. Higher magnifications of *O-fut1*⁻ cells are shown in the small panels at right (B-F). Clone boundaries are indicated by white dashed lines (A-E).

PDI-GFP was detected with the mouse anti-GFP primary antibody and two different fluorescent secondary antibodies (Fig. 3F), and the pattern of the two fluorescent signals was the same, confirming the resolution of our analysis. The Notch-containing vesicles were also negative for *cis*-Golgi (anti-KDEL receptor) and Golgi (anti-Golgi, *Drosophila*) markers (data not shown). Therefore, our results indicated that most Notch did not accumulate in the conventional ER. However, these results do not exclude the possibility that Notch accumulated in a specialized ER compartment (Huyer et al., 2004).

Enzymatic-activity-independent function of *O-fut1* required for Notch endocytic trafficking

O-fut1 has both *O*-fucosyltransferase-activity-dependent and -independent functions (Okajima et al., 2005). Therefore, we investigated whether the novel function of *O-fut1* in Notch endocytic trafficking depends on its enzymatic activity. As reported, an *O*-fucose-independent function of *O-fut1* can be studied using a mutant of the *GDP-D-mannose 4,6-dehydratase* (*Gmd*) gene, which encodes the first enzyme of the de novo GDP-fucose synthesis pathway (Roos et al., 2002; Okajima et al., 2005). We generated two putative null-mutant alleles of *Gmd* (Fig. 4A). The concentration of GDP-fucose in lysates prepared from the third-instar larvae of *Gmd* mutants was determined biochemically (Fig. 4B). The GDP-fucose level in the *Gmd*^{H78} and *Gmd*^{H43} heterozygotes was approximately half that of wild-type larvae, and it was not detectable in the *Gmd*^{H78} and *Gmd*^{H43} homozygotes (Fig. 4B). These results, which are consistent with these two alleles being null mutations of *Gmd*, corroborate the belief that GDP-fucose is synthesized exclusively from GDP-mannose via the de novo pathway in *Drosophila* (Roos et al., 2002). As reported before, using the *Gmd*^I allele (Okajima et al., 2005), Notch signaling was abolished in the *Gmd*^{H78} wing discs (Fig. 4C,D). However, Engrailed (*En*) expression, which is confined to the posterior compartment of the wing disc, was normal in the *Gmd*^{H78} wing disc (Fig. 4E,F), supporting the idea that this defect was specific to the Notch signal.

To test whether the defect in Notch endocytic trafficking in *O-fut1*⁻ cells was due to the failure of Notch *O*-fucosylation, we examined the endocytic transportation of Notch in the *Gmd*^{H78} background. By contrast to the result in *O-fut1*⁻ cells (Fig. 2L), we found that Notch was mostly located in the dextran-positive vesicles (98%, *n*=87) in the *Gmd* mutant (Fig. 4G). In addition, Notch did not accumulate to abnormally high levels in the *Gmd* mutant wing discs, although the size of the Notch-containing endocytic vesicles was slightly greater than those observed in wild-type cells (Fig. 4H,I). Nevertheless, this result suggested that the defect in the endocytic trafficking in *O-fut1*⁻ cells occurs independently of the *O*-fucose modification of Notch. To confirm that this defect was not due to a lack of *O*-fucosylation on Notch, we generated somatic *O-fut1*⁻ clones in the *Gmd*^{H78} wing disc. We observed increased Notch protein levels in the *O-fut1*⁻, *Gmd*^{H78} double-mutant cells (Fig. 4J, inside the white dotted line). Therefore, the knockout of *O-fut1* in the *Gmd* mutant still induced the abnormal accumulation of Notch (Fig. 4J), again indicating that this effect is independent of the enzymatic function of *O-fut1*.

O-fut1 promotes the degradation of Notch

Our results suggested that Notch was transported to the plasma membrane and internalized in *O-fut1*⁻ cells, although it was not delivered to the early endosomes in these cells. In addition, our live-tissue labeling experiments showed that Notch became stable in endocytic vesicles after its incorporation by endocytosis in *O-fut1*⁻ cells (Fig. 2K). Thus, it is likely that Notch failed to be delivered to

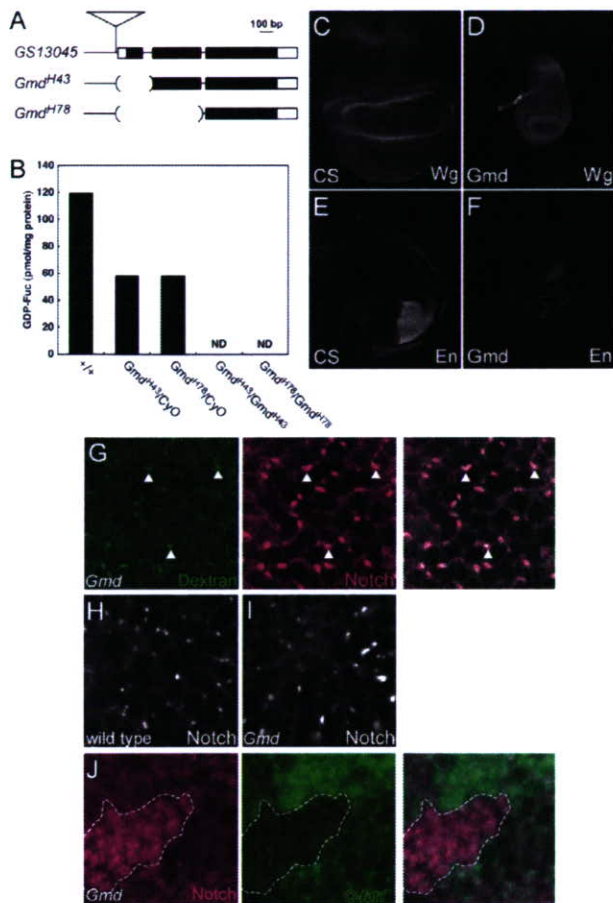


Fig. 4. O-fut1 was required for the endocytic transportation of Notch in a manner independent of its enzymatic activity.

(A) Genomic organization of the *Gmd* locus. Exons are shown as boxes, and the predicted coding region is in black. The regions 3' to the P-element insertion site of *GS13045* are deleted in *Gmd*^{H43} (~0.4 kb) and *Gmd*^{H78} (~0.8 kb). (B) Concentration of GDP-fucose in *Gmd* mutant larvae was measured in duplicate. ND, not detected. (C-F) Wild-type (C,E) and *Gmd*^{H78} homozygous (D,F) wing discs stained with anti-Wg (C,D) and anti-En antibodies (E,F). (G) Uptake of fluorescent dextran by live *Gmd*^{H78} homozygous mutant wing discs after a 10 minute incubation and a 20 minute chase at 25°C. Dextran and Notch are shown in green and magenta, respectively. Some dextran-positive vesicles are indicated by arrowheads. (H,I) Notch staining in wild-type (H) and *Gmd*^{H78} (I) wing discs. (J) *O-fut1*⁻ clones generated in *Gmd*^{H78} wing discs, then stained with anti-Notch (magenta) and anti-myc (clone marker, green) antibodies. The clone boundary is indicated by a white dashed line. All wing discs were isolated from late third-instar larvae.

the lysosomes, where it is normally degraded in these cells (Lu and Bilder, 2005). We therefore speculated that the turnover of Notch is reduced in the *O-fut1*⁻ cells. To address this possibility, we examined the half-life of Notch in wild-type and *O-fut1*⁻ cells. We used a heat-shock-inducible Notch-GAL4 fusion protein, N⁺-GV3, which retains the wild-type function of Notch (Struhl and Adachi, 1998). The N⁺-GV3, which is produced for a short period under the control of a heat-shock promoter, can be specifically detected by an anti-GAL4 antibody (Struhl and Adachi, 1998). Thus, we could trace the

fates of this Notch protein against the background of continuously produced endogenous Notch (Hori et al., 2004). Thirty minutes after heat shock, N⁺-GV3 was expressed uniformly throughout the wing disc (Fig. 5B). Although the N⁺-GV3 was gradually degraded, there was more N⁺-GV3 in the *O-fut1*⁻ cells 6 and 12 hours after heat shock than in the surrounding wing disc cells (Fig. 5C,D).

As O-fut1 is thought to act extracellularly (Haines and Irvine, 2003), we next examined the requirement for the Notch extracellular domain for its stabilization in the *O-fut1*⁻ clones. N⁺-GF-GV3, a *Drosophila* Notch derivative lacking the fifth to 23rd (of 36) Notch EGF-like repeats (Struhl and Adachi, 1998; Artavanis-Tsakonas et al., 1999), showed no increased stability in the *O-fut1*⁻ clones (Fig. 5E). Therefore, the Notch EGF repeats seem to be essential for the stabilization of Notch in *O-fut1*⁻ cells.

Because the half-life of Notch was prolonged in *O-fut1*⁻ cells, we tested whether O-fut1 overexpression would promote Notch degradation. O-fut1 overexpression was driven by *UAS-O-fut1* under the control of *en-GAL4* (Fig. 5F-H). N⁺-GV3 expression was induced by heat shock and detected with anti-GAL4 antibodies, as above. Although the anti-GAL4 antibody also recognized the GAL4 generated from *en-GAL4*, the GAL4 staining remained at the background level under our conditions (Fig. 5F). We found that N⁺-GV3 was greatly decreased in the O-fut1-overexpressing cells compared with the wild-type cells 24 hours after heat shock (Fig. 5H). Therefore, as opposed to the loss of O-fut1 function, its overexpression promoted the degradation of Notch. O-fut1-G3, which has three amino acid substitutions in an essential motif for glycosyltransferase activity, lacks enzymatic activity [Nti-G3 in Sasamura et al. (Sasamura et al., 2003)]. Significantly, O-fut1-G3 promoted the degradation of Notch as efficiently as did wild-type O-fut1 (compare Fig. 5H,I), further supporting our idea that O-fut1 promotes the transportation of Notch to the lysosomes independent of Notch O-fucosylation.

Because a lack of O-fut1 activity results in the failure of Notch-ligand interactions (Sasamura et al., 2003; Okajima et al., 2003), it is difficult to study the consequences of the disturbance in Notch turnover using loss-of-function mutations of *O-fut1*. Therefore, to examine the possible role of the O-fut1-regulated Notch turnover in the developmental context, we resorted to overexpression studies. The overexpression of O-fut1 or O-fut1-G3 in wing discs caused wing-nicking and vein-thickening phenotypes (Fig. 5J-L) that were reminiscent of Notch loss-of-function phenotypes (de Celis and Garcia-Bellido, 1994). The expression of *wingless* (*wg*), a target of Notch signaling in the wing disc, was reduced significantly in the O-fut1-overexpressing wing disc (Fig. 5M,N) (Rulifson and Blair, 1995). Additional consistent evidence is the finding that O-fut1 overexpression represses Notch signaling in notal microchaete development (Okajima and Irvine, 2002). These results suggest that O-fut1 downregulates Notch signaling by promoting the degradation of Notch via an O-fucosylation-independent mechanism.

O-fut1 interacts with the extracellular domain of Notch

O-fut1 has a KDEL-like motif, a HEEL sequence, at its C-terminus, which probably acts as an ER-retention signal (Teasdale and Jackson, 1996). Indeed, it was reported that O-fut1 mostly localizes to the ER (Okajima et al., 2005). However, given that O-fut1 influences the endocytic trafficking of Notch, it is likely that at least some fraction of O-fut1 is transported to the plasma membrane and then incorporated into the cells. Garland cells are suitable to study the subcellular localization of proteins *in vivo* because of their large cytoplasm (Culi and Mann, 2003). In these cells, we found Myc-

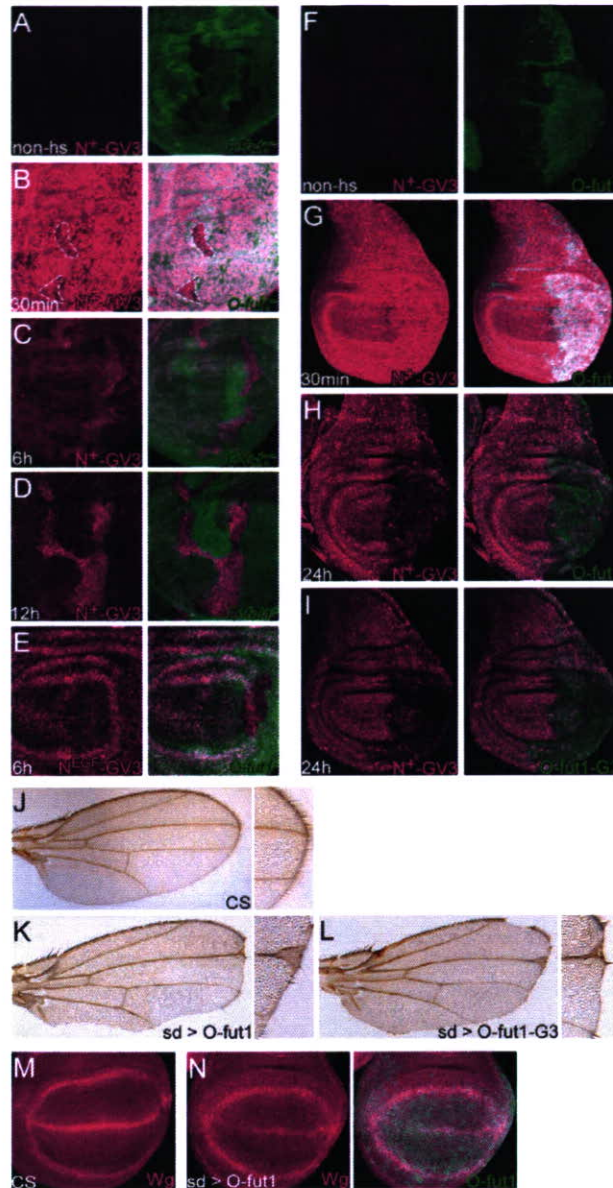


Fig. 5. Notch turnover is modulated by O-fut1. (A-D) The expression of N⁺-GV3 (magenta) was induced by a 1 hour heat shock at 37°C (B-D) or was not induced (A), and the wing discs were subsequently incubated at room temperature for another 30 minutes (B), 6 hours (C) or 12 hours (D). *O-fut1*⁻ clones are denoted by the absence of GFP (green). The clone boundaries are indicated by white dashed lines in (B). (E) Expression of a mutant form of N⁺-GV3 (N⁺-GV3^{EGF}, magenta), which lacks the fifth to 23rd EGF-like repeats, was induced by a 1 hour heat shock followed by a 6 hour incubation at room temperature. *O-fut1*⁻ clones lack GFP (green). (F-I) O-fut1 (F-H) or O-fut1-G3 (I) driven by *en-GAL4* were overexpressed (green) in the posterior compartment of wing discs, and N⁺-GV3 expression (magenta) was induced by a 3 hour heat shock at 37°C (G-I) or was not induced (F). Wing discs were dissected 30 minutes (G) or 24 hours (H,I) after heat shock. (J-L) Adult wings. (J) Wild-type. (K,L) Wing phenotype induced by the overexpression of wild-type O-fut1 (K) or O-fut1-G3 (L) driven by *sd-GAL4*. Higher magnification images of the wing margin are shown at right. (M,N) *wg* expression (magenta) was detected in the wild-type wing disc (M) or the wing disc overexpressing *O-fut1* (green) under the control of *sd-GAL4* (N). The right panel of N shows a merged image of Wg and O-fut1 expression. All wing discs were isolated from late third-instar larvae.

To test our hypothesis that O-fut1 functions during Notch endocytosis, we investigated whether extracellular O-fut1 was incorporated into cells by endocytosis and whether it could rescue the defects in Notch endocytosis associated with the knockdown of O-fut1 function. S2 cells expressing Notch were cultured with conditioned medium containing secreted Myc-tagged O-fut1 (O-fut1-ER⁻). We detected the O-fut1-ER⁻, which was added extracellularly, in vesicles in cells expressing Notch, but not in control cells (Fig. 6D). In the Notch-expressing cells, Notch and O-fut1-ER⁻ were co-localized in the vesicles (Fig. 6D). In addition, the extracellularly added O-fut1 suppressed the defects in the endocytic transportation of Notch that were induced by the inhibition of O-fut1 function. In the control S2 cells, about 18% of the Notch-containing vesicles co-localized with Hrs (Fig. 6E,H). The co-expression of a double-stranded RNA corresponding to O-fut1 mRNA [O-fut1-IR; *nti*-IR in Sasamura et al. (Sasamura et al., 2003)] suppressed this co-localization to about 8.5% (Fig. 6F,H). Importantly, the extracellularly added O-fut1 was sufficient to rescue Notch co-localization with Hrs to 16.7% (Fig. 6G,H). Furthermore, we found that O-fut1-ER⁻ was secreted more efficiently into the medium (data not shown) (Okajima et al., 2005) and accelerated the degradation of N⁺-GV3 more strongly than native O-fut1 in vivo (Fig. 6I,J). In addition, the overexpression of O-fut1-ER⁻ induced more severe Notch loss-of-function phenotypes than did overexpressed wild-type O-fut1 (Fig. 6K,L). Together, these results support the idea that the acceleration of Notch turnover, which is induced by extracellular O-fut1, leads to the downregulation of Notch signaling.

O-fut1 is required for the constitutive trafficking of Notch

Ligand binding can force a receptor to choose a specific trafficking path (Sorkin and Von Zastrow, 2002). Therefore, it is possible that extracellular O-fut1 is required for Notch-ligand interactions, which may trigger the transportation of Notch to the endosome. However, no accumulation of Notch was seen in the somatic clones of cells that were double mutants for *Delta* and *Serrate*, as

tagged O-fut1, which is otherwise wild type [O-fut1-myc; Nti-myc in Sasamura et al. (Sasamura et al., 2003)], in small vesicles, probably exocytic ones, that were not labeled with ER or Golgi markers (Fig. 6A,A'; data not shown). Some of the punctate O-fut1 staining co-localized with N⁺-GV3 staining, which was located in vesicles distant from the peri-nuclear ER (Fig. 6B,B', arrows). These results suggest that O-fut1 physically interacts with Notch during exocytosis and/or endocytosis in vivo. Indeed, O-fut1 forms a stable complex with Notch, as shown by immunoprecipitation, which has been proposed to account for the enzymatic-activity-independent functions of O-fut1 (Fig. 6C) (Okajima et al., 2005). We also found that a Notch derivative lacking the EGF-like repeats (Notch^{ΔEC}) did not co-precipitate with O-fut1 (Fig. 6C). These results suggest that O-fut1 interacted with the EGF-like repeats of the Notch extracellular domain.

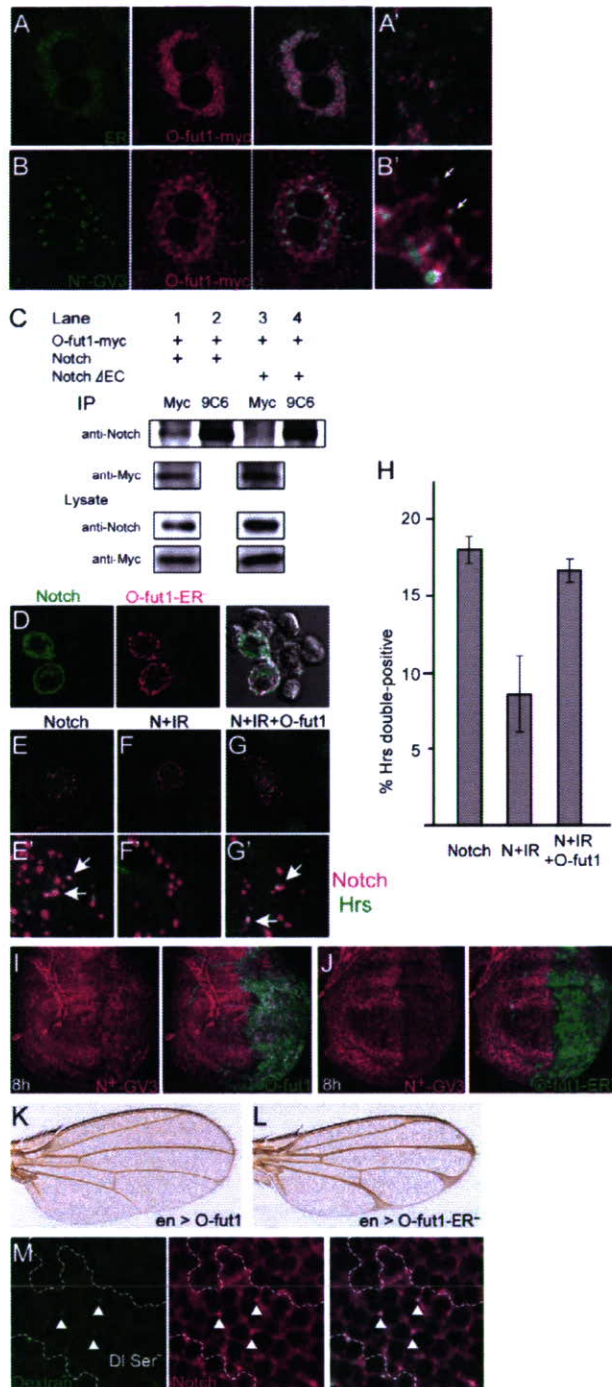


Fig. 6. O-fut1 is secreted and internalized by cells.

(A,B) Intracellular localization of O-fut1 was examined in Garland cells overexpressing either ER-CFP (A, green) or N⁺-GV3 (B, green) and O-fut1-myc (A,B, magenta). ER-CFP and O-fut1-myc were driven by *da-GAL4*, and N⁺-GV3 was induced by a 2 hour heat shock that ended 30 minutes before fixation. (A',B') Higher magnifications of A and B, respectively. Arrows indicate O-fut1 and Notch double-positive vesicles, which were distant from the peri-nuclear ER (B'). (C) S2 cells were transfected with the expression constructs for O-fut1-myc and Notch (lanes 1,2), or Notch Δ EC (lanes 3,4). Lysates prepared from these cells were immunoprecipitated using anti-Myc (lanes 1,3) or anti-Notch (lanes 2,4) antibodies, and the blots were probed with the anti-Notch antibody (C17.9C6) or anti-Myc antibody (9E10). The expression of Notch and O-fut1 in the lysates was confirmed by western blot (Lysate, lower panels). (D) O-fut1 was incorporated into cells in a Notch-dependent manner. S2 cells expressing Notch (green) were incubated with the O-fut1-ER⁻ protein (magenta). The brightfield image is superimposed in the right panel. (E-H) The endocytosis defect in the O-fut1 knockdown cells was rescued by the addition of extracellular O-fut1. S2 cells expressing Notch (E) or Notch and O-fut1-IR (F,G) were incubated with anti-Notch antibody (rat1, magenta), fixed, and co-stained with anti-Hrs antibody (green). (G) Live cells expressing Notch and O-fut1-IR were incubated with O-fut1-ER⁻ for 20 minutes before the addition of anti-Notch antibody. (E'-G') Corresponding higher magnification images of E-G. Arrows indicate Notch and Hrs double-positive vesicles. (H) Average ratio of Notch and Hrs double-positive vesicles shown as the percentage of Notch-positive vesicles. Mean \pm s.d. from triplicate assays (more than 20 cells each) are shown. (I,J) The N⁺-GV3 protein (magenta) 8 hours after heat shock for 1 hour in third-instar wing discs overexpressing O-fut1 (I) or O-fut1-ER⁻ (J) (green) driven by *en-GAL4*. (K,L) Adult wings. O-fut1 (K) and O-fut1-ER⁻ (L) were overexpressed under the control of *en-GAL4*, and the resulting wing phenotypes were examined. (M) Fluorescent dextran uptake by *Delta* and *Serrate* double-mutant cells in live wing discs after a 10 minute incubation and a 20 minute chase at 25°C. Clone boundary and dextran-positive vesicles are indicated by dotted lines and white arrowheads, respectively. All wing discs were isolated from late third-instar larvae.

DISCUSSION

O-fut1 is a novel extracellular component required for Notch endocytic trafficking

As a novel and enzymatic-activity-independent function of O-fut1, we propose that O-fut1 is required for the constitutive endocytic trafficking of Notch from the plasma membrane to the early endosome. Previously, it was shown that O-fut1 acts as a specific chaperon for Notch in an enzymatic-activity-independent manner (Okajima et al., 2005). Thus, O-fut1 has two distinct roles, neither of which depend on the O-fucosylation of Notch, during either the exocytotic or endocytic transportation of Notch.

As evidence for the chaperon activity of O-fut1, it was reported that Notch accumulates in the ER in *O-fut1*⁻ cells (Okajima et al., 2005). The idea that O-fut1 acts as a chaperon was based on the assumption that its absence results in mis-folded Notch, which could be retained in the ER by quality control mechanisms. However, our results suggested that the level of apical surface Notch, which was recognized by live tissue staining with an anti-Notch antibody, was not reduced significantly. Therefore, at least some Notch is delivered to the plasma membrane in *O-fut1*⁻ cells. This Notch transportation may be slower or less efficient in these cells, which could account for the previous observation that Notch did not reach the surface of O-fut1-depleted *Drosophila* S2 cells at a given time point (Okajima

previously reported (data not shown) (Okajima et al., 2005). In addition, Notch co-localized normally with dextran added extracellularly to these double-mutant cells, indicating there was no interference with the endocytic transportation of Notch (Fig. 6M). Therefore, O-fut1 is probably required for the constitutive vesicular transportation of Notch, rather than for its ligand-induced endocytic transportation.

et al., 2005). In addition, our high-resolution analysis revealed that Notch did not accumulate in vesicles that were positive for two well-characterized ER markers, although we could not exclude the possibility that Notch accumulates in a specific ER subdomain (Huyer et al., 2004). However, biochemical evidence indicates that O-fut1 promotes the proper folding of Notch (Okajima et al., 2005). Thus, we speculate that the two enzymatic-activity-independent roles of O-fut1 are not mutually exclusive and can take place simultaneously.

O-fut1 is required for the transportation of Notch to the early endosome

Our results showed that Notch failed to be delivered to the Hrs-positive early endosomes in *O-fut1*⁻ cells. Therefore, we speculate that O-fut1 may be required for the early endosomal fusion of endocytic vesicles containing Notch, because Notch was internalized in small vesicles in *O-fut1*⁻ cells, but was not transported to the early endosomes. Indeed, similar Notch accumulation in small vesicles is observed in cells with defective endosome vesicle fusion caused by a mutation in the *avl* gene (Lu and Bilder, 2005). However, in the present study, we were unable to determine the nature of the vesicles where Notch was accumulated in *O-fut1*⁻ cells, because the available markers for ER, Golgi, early endosomes, recycling endosomes, late endosomes and lysosomes did not colocalize with the accumulated Notch.

Degradation of transmembrane proteins in the lysosome requires the proteins to be transported first to the early and then to the late endosome (Babst, 2005). Thus, our model predicts that the half-life of Notch is prolonged in *O-fut1*⁻ cells, because Notch was not transported to the early endosome in these cells. Consistent with this model, we found that the half-life of Notch was extended in *O-fut1*⁻ cells and reduced in cells overexpressing O-fut1. In addition, the overexpression of O-fut1 suppressed Notch signaling in vivo. Therefore, O-fut1 may play an important role in maintaining the appropriate Notch turnover ratio, which probably functions to downregulate Notch signaling in wild-type cells.

We also found that Notch did not accumulate in the cells that were double mutants for *Delta* and *Serrate*, suggesting that interactions between Notch and its ligands are not relevant to the O-fut1-dependent endocytosis of Notch. Therefore, the accumulation of Notch in *O-fut1*⁻ cells is due to defects in constitutive endocytosis rather than in ligand-induced endocytosis. Taking these results together, we speculate that O-fut1 may be involved in sweeping unactivated and excess Notch from the plasma membrane under physiological conditions. Therefore, the lack of this O-fut1 function predictably results in the upregulation of Notch signaling. Our overexpression analysis of O-fut1 is consistent with this idea. However, it is difficult to examine this possibility using loss-of-function mutants of *O-fut1*, because O-fut1 is also essential for the interactions between Notch and its ligands (Sasamura et al., 2003; Okajima et al., 2003).

O-fut1 functions cell autonomously in the endocytic transportation of Notch

Although O-fut1 is known to be secreted when it is expressed in S2 cells (Okajima et al., 2005), we found that the function of O-fut1 was required in a cell-autonomous manner in vivo. The accumulation of Notch was observed in all *O-fut1*⁻ cells in somatic clones, even in cells surrounded by wild-type cells (arrow in Fig. 1B,C). Therefore, under physiological conditions, O-fut1 is probably transported to the plasma membrane and then endocytosed only into the same cell. In wild-type cells, O-fut1 may continuously interact with Notch as it

cycles from exocytic to endocytic pathways. The following three observations support this idea. First, O-fut1 forms a stable complex with the extracellular domain of Notch. Second, O-fut1 and Notch were occasionally found in the same exocytic vesicles. Third, O-fut1 added extracellularly was incorporated into the cells in a Notch-dependent manner. However, we also found that O-fut1 added to the medium was sufficient to restore the endocytosis of Notch in O-fut1 knockdown cells. Therefore, the interaction of O-fut1 and Notch, which occurs after Notch reaches the cell surface, is sufficient for the normal endocytic trafficking of Notch. However, it is presently unknown how extracellular interactions between Notch and O-fut1 affect the endocytic trafficking of Notch. The specific complex of the Notch extracellular domain and O-fut1 may influence the intracellular recognition machinery between Notch-containing early endocytic vesicles and the early endosomes, such as the tethering factors or Rab5 (Rodriguez-Boulán et al., 2005). Nevertheless, our results raise the interesting possibility that extracellular modification enzymes may be necessary for, or control, the endocytic transportation path of receptor proteins that are also their substrates.

We thank G. Struhl, A. K. Sato, H. J. Bellen, M. Gonzalez-Gaitan, N. Perrimon, the Bloomington Drosophila Stock Center, and the Developmental Studies Hybridoma Bank for providing fly stocks and antibodies. We also thank S. Artavanis-Tsakonas and A. Mukherjee for critical comments on the manuscript, and T. Okajima, K. D. Irvine, E. Spana, D. Bilder and N. Perrimon for support during the early stages of this work. This work was supported by grants-in-aid from the Japanese Ministry of Education, Culture, Sports and Science (K.M.), and PRESTO, JST (K.M.).

References

- Artavanis-Tsakonas, S., Rand, M. D. and Lake, R. J. (1999). Notch signaling: cell fate control and signal integration in development. *Science* **284**, 770-776.
- Babst, M. (2005). A protein's final ESCRT. *Traffic* **6**, 2-9.
- Berdnik, D., Torok, T., Gonzalez-Gaitan, M. and Knoblich, J. A. (2002). The endocytic protein α -Adaptin is required for numb-mediated asymmetric cell division in *Drosophila*. *Dev. Cell* **3**, 221-231.
- Bobinac, Y., Marcellou, C., Morin, X. and Debrec, A. (2003). Dynamics of the endoplasmic reticulum during early development of *Drosophila melanogaster*. *Cell Motil. Cytoskeleton* **54**, 217-225.
- Bray, S. and Furiols, M. (2001). Notch pathway: making sense of Suppressor of Hairless. *Curr. Biol.* **11**, R217-R221.
- Brook, W. J. and Cohen, S. M. (1996). Antagonistic interactions between wingless and decapentaplegic responsible for dorsal-ventral pattern in the *Drosophila* leg. *Science* **273**, 1373-1377.
- Brückner, K., Perez, L., Clausen, H. and Cohen, S. (2000). Glycosyltransferase activity of Fringe modulates Notch-Delta interactions. *Nature* **406**, 411-415.
- Chang, H. C., Newmyer, S. L., Hull, M. J., Ebersold, M., Schmid, S. L. and Mellman, I. (2002). Hsc70 is required for endocytosis and clathrin function in *Drosophila*. *J. Cell Biol.* **159**, 477-487.
- Culi, J. and Mann, R. S. (2003). Boca, an endoplasmic reticulum protein required for wingless signaling and trafficking of LDL receptor family members in *Drosophila*. *Cell* **112**, 343-354.
- de Celis, J. F. and Garcia-Bellido, A. (1994). Roles of the *Notch* gene in *Drosophila* wing morphogenesis. *Mech. Dev.* **46**, 109-122.
- Dollar, G., Struckhoff, E., Michaud, J. and Cohen, R. S. (2002). Rab11 polarization of the *Drosophila* oocyte: a novel link between membrane trafficking, microtubule organization, and *oskar* mRNA localization and translation. *Development* **129**, 517-526.
- Entchev, E. V., Schwabedissen, A. and González-Gaitán, M. (2000). Gradient formation of the TGF- β homolog Dpp. *Cell* **103**, 981-991.
- Fehon, R. G., Kooh, P. J., Rebay, I., Regan, C. L., Xu, T., Muskavitch, M. A. and Artavanis-Tsakonas, S. (1990). Molecular interactions between the protein products of the neurogenic loci *Notch* and *Delta*, two EGF-homologous genes in *Drosophila*. *Cell* **61**, 523-534.
- Fehon, R. G., Johansen, K., Rebay, I. and Artavanis-Tsakonas, S. (1991). Complex cellular and subcellular regulation of Notch expression during embryonic and imaginal development of *Drosophila*: implications for Notch function. *J. Cell Biol.* **113**, 657-669.
- Ferrari, D. M. and Söling, H. D. (1999). The protein disulphide-isomerase family: unravelling a string of folds. *Biochem. J.* **339**, 1-10.
- Fleming, R. J. (1998). Structural conservation of Notch receptors and ligands. *Semin. Cell Dev. Biol.* **9**, 599-607.
- Giebel, B. and Wodarz, A. (2006). Tumor suppressors: control of signaling by endocytosis. *Curr. Biol.* **16**, R91-R92.

- Goto, S., Taniguchi, M., Muraoka, M., Toyoda, H., Sado, Y., Kawakita, M. and Hayashi, S. (2001). UDP-sugar transporter implicated in glycosylation and processing of Notch. *Nat. Cell Biol.* **3**, 816-822.
- Haines, N. and Irvine, K. D. (2003). Glycosylation regulates Notch signalling. *Nat. Rev. Mol. Cell Biol.* **4**, 786-797.
- Herz, H. M., Chen, Z., Scherr, H., Lackey, M., Bolduc, C. and Bergmann, A. (2006). *vps25* mosaics display non-autonomous cell survival and overgrowth, and autonomous apoptosis. *Development* **133**, 1871-1880.
- Hori, K., Fostier, M., Ito, M., Fuwa, T. J., Go, M. J., Okano, H., Baron, M. and Matsuno, K. (2004). *Drosophila* Deltex mediates Suppressor of Hairless-independent and late-endosomal activation of Notch signaling. *Development* **131**, 5527-5537.
- Huyer, G., Longworth, G. L., Mason, D. L., Mallampalli, M. P., McCaffery, J. M., Wright, R. L. and Michaelis, S. (2004). A striking quality control subcompartment in *Saccharomyces cerevisiae*: the endoplasmic reticulum-associated compartment. *Mol. Biol. Cell* **15**, 908-921.
- Jékely, G. and Rørth, P. (2003). Hrs mediates downregulation of multiple signalling receptors in *Drosophila*. *EMBO Rep.* **4**, 1163-1168.
- Johnson, R. L., Grenier, J. K. and Scott, M. P. (1995). *patched* overexpression alters wing disc size and pattern: transcriptional and post-transcriptional effects on *hedgehog* targets. *Development* **121**, 4161-4170.
- Kidd, S., Lockett, T. J. and Young, M. W. (1983). The Notch locus of *Drosophila melanogaster*. *Cell* **34**, 421-433.
- Kopito, R. R. (2000). Aggresomes, inclusion bodies and protein aggregation. *Trends Cell Biol.* **10**, 524-530.
- Lai, E. C. (2004). Notch signaling: control of cell communication and cell fate. *Development* **131**, 965-973.
- Le Borgne, R. and Schweisguth, F. (2003). Unequal segregation of Neuralized biases Notch activation during asymmetric cell division. *Dev. Cell* **5**, 139-148.
- Le Borgne, R., Bardin, A. and Schweisguth, F. (2005). The roles of receptor and ligand endocytosis in regulating Notch signaling. *Development* **132**, 1751-1762.
- Lee, T. and Luo, L. (1999). Mosaic analysis with a repressible cell marker for studies of gene function in neuronal morphogenesis. *Neuron* **22**, 451-461.
- Ligoxygakis, P., Yu, S. Y., Delidakis, C. and Baker, N. E. (1998). A subset of Notch functions during *Drosophila* eye development require *Su(H)* and the *E(spl)* gene complex. *Development* **125**, 2893-2900.
- Lloyd, T. E., Atkinson, R., Wu, M. N., Zhou, Y., Pennetta, G. and Bellen, H. J. (2002). Hrs regulates endosome membrane invagination and tyrosine kinase receptor signaling in *Drosophila*. *Cell* **108**, 261-269.
- Lu, H. and Bilder, D. (2005). Endocytic control of epithelial polarity and proliferation in *Drosophila*. *Nat. Cell Biol.* **7**, 1132-1139.
- Maitra, S., Kulikaukas, R. M., Gavilan, H. and Fehon, R. G. (2006). The tumor suppressors merlin and expanded function cooperatively to modulate receptor endocytosis and signaling. *Curr. Biol.* **16**, 702-709.
- Matsuno, K., Ito, M., Hori, K., Miyashita, F., Suzuki, S., Kishi, N., Artavanis-Tsakonas, S. and Okano, H. (2002). Involvement of a proline-rich motif and RING-H2 finger of Deltex in the regulation of Notch signaling. *Development* **129**, 1049-1059.
- Moberg, K. H., Schelble, S., Burdick, S. K. and Hariharan, I. K. (2005). Mutations in *erupted*, the *Drosophila* ortholog of mammalian tumor susceptibility gene 101, elicit non-cell-autonomous overgrowth. *Dev. Cell* **9**, 699-710.
- Moloney, D. J., Panin, V. M., Johnston, S. H., Chen, J., Shao, L., Wilson, R., Wang, Y., Stanley, P., Irvine, K. D., Haltiwanger, R. S. et al. (2000). Fringe is a glycosyltransferase that modifies Notch. *Nature* **406**, 369-375.
- Mukherjee, A., Veraksa, A., Bauer, A., Rosse, C., Camonis, J. and Artavanis-Tsakonas, S. (2005). Regulation of Notch signalling by non-visual beta-arrestin. *Nat. Cell Biol.* **7**, 1191-1201.
- Mumm, J. S. and Kopan, R. (2000). Notch signaling: from the outside in. *Dev. Biol.* **228**, 151-165.
- Noda, K., Miyoshi, E., Nakahara, S., Ihara, H., Gao, C. X., Honke, K., Yanagidani, S., Sasaki, Y., Kasahara, A., Hori, M. et al. (2002). An enzymatic method of analysis for GDP-L-fucose in biological samples, involving high-performance liquid chromatography. *Anal. Biochem.* **310**, 100-106.
- Noda, K., Miyoshi, E., Gu, J., Gao, C.-X., Nakahara, S., Kitada, T., Honke, K., Suzuki, K., Yoshihara, H., Yoshikawa, K. et al. (2003). Relationship between elevated FX expression and increased production of GDP-L-fucose, a common donor substrate for fucosylation in human hepatocellular carcinoma and hepatoma cell lines. *Cancer Res.* **63**, 6282-6289.
- Oda, H., Uemura, T., Harada, Y., Iwai, Y. and Takeichi, M. (1994). A *Drosophila* homolog of cadherin associated with armadillo and essential for embryonic cell-cell adhesion. *Dev. Biol.* **165**, 716-726.
- Okajima, T. and Irvine, K. D. (2002). Regulation of Notch signaling by O-linked fucose. *Cell* **111**, 893-904.
- Okajima, T., Xu, A. and Irvine, K. D. (2003). Modulation of Notch-ligand binding by protein O-fucosyltransferase 1 and Fringe. *J. Biol. Chem.* **278**, 42340-42345.
- Okajima, T., Xu, A., Lei, L. and Irvine, K. D. (2005). Chaperone activity of protein O-fucosyltransferase 1 promotes Notch receptor folding. *Science* **307**, 1599-1603.
- Panin, V. M., Papayannopoulos, V., Wilson, R. and Irvine, K. D. (1997). Fringe modulates Notch-ligand interactions. *Nature* **387**, 908-912.
- Patel, N. H., Martin-Blanco, E., Coleman, K. G., Poole, S. J., Ellis, M. C., Kornberg, T. B. and Goodman, C. S. (1989). Expression of *engrailed* proteins in arthropods, annelids, and chordates. *Cell* **58**, 955-968.
- Rebay, I., Fleming, R. J., Fehon, R. G., Cherbass, L., Cherbass, P. and Artavanis-Tsakonas, S. (1991). Specific EGF repeats of Notch mediate interactions with Delta and Serrate: implications for Notch as a multifunctional receptor. *Cell* **67**, 687-699.
- Rodriguez-Boulan, E., Kreitzer, G. and Musch, A. (2005). Organization of vesicular trafficking in epithelia. *Nat. Rev. Mol. Cell Biol.* **6**, 233-247.
- Roos, C., Kolmer, M., Mattila, P. and Renkonen, R. (2002). Composition of *Drosophila melanogaster* proteome involved in fucosylated glycan metabolism. *J. Biol. Chem.* **277**, 3168-3175.
- Roy, S., Shashidhara, L. S. and VijayRaghavan, K. (1997). Muscles in the *Drosophila* second thoracic segment are patterned independently of autonomous homeotic gene function. *Curr. Biol.* **7**, 222-227.
- Rulifson, E. J. and Blair, S. S. (1995). Notch regulates *wingless* expression and is not required for reception of the paracrine *wingless* signal during wing margin neurogenesis in *Drosophila*. *Development* **121**, 2813-2824.
- Sakata, T., Sakaguchi, H., Tsuda, L., Higashitani, A., Aigaki, T., Matsuno, K. and Hayashi, S. (2004). *Drosophila* Nedd4 regulates endocytosis of Notch and suppresses its ligand-independent activation. *Curr. Biol.* **14**, 2228-2236.
- Sasamura, T., Sasaki, N., Miyashita, F., Nakao, S., Ishikawa, H. O., Ito, M., Kitagawa, M., Harigaya, K., Spana, E., Bilder, D. et al. (2003). *neurotic*, a novel maternal neurogenic gene, encodes an O-fucosyltransferase that is essential for Notch-Delta interactions. *Development* **130**, 4785-4795.
- Selva, E. M., Hong, K., Baeg, G. H., Beverley, S. M., Turco, S. J., Perrimon, N. and Häcker, U. (2001). Dual role of the *fringe* connection gene in both heparan sulphate and fringe-dependent signalling events. *Nat. Cell Biol.* **3**, 809-815.
- Seugnet, L., Simpson, P. and Haenlin, M. (1997). Requirement for dynamin during Notch signaling in *Drosophila* neurogenesis. *Dev. Biol.* **192**, 585-598.
- Shi, S. and Stanley, P. (2003). Protein O-fucosyltransferase 1 is an essential component of Notch signaling pathways. *Proc. Natl. Acad. Sci. USA* **100**, 5234-5239.
- Sorkin, A. and Von Zastrow, M. (2002). Signal transduction and endocytosis: close encounters of many kinds. *Nat. Rev. Mol. Cell Biol.* **3**, 600-614.
- Struhl, G. and Adachi, A. (1998). Nuclear access and action of Notch in vivo. *Cell* **93**, 649-660.
- Teasdale, R. D. and Jackson, M. R. (1996). Signal-mediated sorting of membrane proteins between the endoplasmic reticulum and the golgi apparatus. *Annu. Rev. Cell Dev. Biol.* **12**, 27-54.
- Thompson, B. J., Mathieu, J., Sung, H. H., Loeser, E., Rørth, P. and Cohen, S. M. (2005). Tumor suppressor properties of the ESCRT-II complex component Vps25 in *Drosophila*. *Dev. Cell* **9**, 711-720.
- Toba, G., Ohsako, T., Miyata, N., Ohtsuka, T., Seong, K. H. and Aigaki, T. (1999). The gene search system: a method for efficient detection and rapid molecular identification of genes in *Drosophila melanogaster*. *Genetics* **151**, 725-737.
- Ullrich, O., Reinsch, S., Urbe, S., Zerial, M. and Parton, R. G. (1996). Rab11 regulates recycling through the pericentriolar recycling endosome. *J. Cell Biol.* **135**, 913-924.
- Vaccari, T. and Bilder, D. (2005). The *Drosophila* tumor suppressor *vps25* prevents nonautonomous overproliferation by regulating notch trafficking. *Dev. Cell* **9**, 687-698.
- Wang, Y., Shao, L., Shi, S., Harris, R. J., Spellman, M. W., Stanley, P. and Haltiwanger, R. S. (2001). Modification of epidermal growth factor-like repeats with O-fucose. Molecular cloning and expression of a novel GDP-fucose protein O-fucosyltransferase. *J. Biol. Chem.* **276**, 40338-40345.
- Wharton, K. A., Johansen, K. M., Xu, T. and Artavanis-Tsakonas, S. (1985). Nucleotide sequence from the neurogenic locus *Notch* implies a gene product that shares homology with proteins containing EGF-like repeats. *Cell* **43**, 567-581.
- Wilkin, M. B., Carbery, A. M., Fostier, M., Aslam, H., Mazaleyrat, S. L., Higgs, J., Myat, A., Evans, D. A., Cornell, M. and Baron, M. (2004). Regulation of Notch endosomal sorting and signaling by *Drosophila* Nedd4 family proteins. *Curr. Biol.* **14**, 2237-2244.
- Wodarz, A., Hinz, U., Engelbert, M. and Knust, E. (1995). Expression of crumbs confers apical character on plasma membrane domains of ectodermal epithelia of *Drosophila*. *Cell* **82**, 67-76.
- Xu, T. and Rubin, G. M. (1993). Analysis of genetic mosaics in developing and adult *Drosophila* tissues. *Development* **117**, 1223-1237.

Carbohydrate Binding Specificity of a Fucose-specific Lectin from *Aspergillus oryzae*

A NOVEL PROBE FOR CORE FUCOSE*[‡]

Received for publication, February 8, 2007, and in revised form, March 23, 2007. Published, JBC Papers in Press, March 23, 2007, DOI 10.1074/jbc.M701195200

Kengo Matsumura^{†1}, Katsuya Higashida[‡], Hiroki Ishida[‡], Yoji Hata[‡], Kenji Yamamoto[§], Masaki Shigeta[¶], Yoko Mizuno-Horikawa[¶], Xiangchun Wang[¶], Eiji Miyoshi[¶], Jianguo Gu^{||}, and Naoyuki Taniguchi^{**}

From the [†]Research Institute, Gekkeikan Sake Company Ltd., 300 Katahara-cho, Fushimi-ku, Kyoto 612-8361, Japan, the [§]Division of Integrated Life Science, Graduate School of Biostudies, Kyoto University, Oiwake-cho, Kitashirakawa Sakyo-ku, Kyoto 606-8502, Japan, the [¶]Department of Biochemistry, Osaka University Graduate School of Medicine, 2-2 Yamadaoka, Suita, Osaka 565-0871, Japan, the ^{||}Division of Regulatory Glycobiology, Institute of Molecular Biomembrane and Glycobiology, Tohoku Pharmaceutical University, 4-4-1 Komatsushima, Aobaku, Sendai, Miyagi 981-8558, Japan, and the ^{**}Department of Disease Glycomics, Research Institute for Microbial Diseases, Osaka University, 2-1 Yamadaoka, Suita, Osaka 565-0871, Japan

The α 1,6-fucosyl residue (core fucose) of glycoproteins is widely distributed in mammalian tissues and is altered under pathological conditions. A probe that specifically detects core fucose is important for understanding the role of this oligosaccharide structure. *Aleuria aurantia* lectin (AAL) and *Lens culinaris* agglutinin-A (LCA) have been often used as carbohydrate probes for core fucose in glycoproteins. Here we show, by using surface plasmon resonance (SPR) analysis, that *Aspergillus oryzae* L-fucose-specific lectin (AOL) has strongest preference for the α 1,6-fucosylated chain among α 1,2-, α 1,3-, α 1,4-, and α 1,6-fucosylated pyridylaminated (PA)-sugar chains. These results suggest that AOL is a novel probe for detecting core fucose in glycoproteins on the surface of animal cells. A comparison of the carbohydrate-binding specificity of AOL, AAL, and LCA by SPR showed that the irreversible binding of AOL to the α 1,2-fucosylated PA-sugar chain (H antigen) relative to the α 1,6-fucosylated chain was weaker than that of AAL, and that the interactions of AOL and AAL with α 1,6-fucosylated glycopeptide (FGP), which is considered more similar to *in vivo* glycoproteins than PA-sugar chains, were similar to their interactions with the α 1,6-fucosylated PA-sugar chain. Furthermore, positive staining of AOL, but not AAL, was completely abolished in the cultured embryo fibroblast (MEF) cells obtained from α 1,6-fucosyltransferase (Fut8) knock-out mice, as assessed by cytological staining. Taken together, these results suggest that AOL is more suitable for detecting core fucose than AAL or LCA.

Lectins are specific carbohydrate-binding or carbohydrate-cross-linking proteins. Many studies have isolated and investigated lectins from a wide range of species including plants, animals and microorganisms. The cell surfaces of organisms are covered with abundant and diverse carbohydrates. Because of

structural diversity, the set of carbohydrates that is expressed on a cell surface has a role in various biological recognition phenomena, including cell-cell interactions, cell-substratum interactions, and metastasis of tumor cells, among others (1). Therefore, some lectins have particular value as specific probes for investigating the distribution, structure and biological function of carbohydrate chains on the cell surface of animal, plant, and microorganism because of their specificity for defined carbohydrate structures (2).

α -L-Fucopyranosyl residues are widely distributed in cell-surface sugar chains and often play important roles in biological phenomena. These residues constitute a part of important antigens, such as the blood group antigen H (3) and stage-specific embryonic antigens (4). Increased levels of fucosyl residues and changes in fucosylation patterns, as a result of different expression levels of various fucosyltransferases, act as specific markers for developmental antigens, particularly in inflammatory processes and in various cancers (5, 6). Furthermore, the α 1,6-fucosylated oligosaccharide content of both liver and serum glycoproteins is elevated during the development of malignant liver diseases because the activity of Fut8 is increased (7). In particular, the sugar chains of α -fetoprotein in serum, a well established tumor marker that is produced by hepatocellular carcinomas, have an abundance of core fucose (8).

To date, some lectins have been identified as fucose-specific including *Lotus tetragonolobus* (3) and *Ulex europaeus* (9) lectins from plants, *Anguilla* lectin from eel (10), *Aleuria aurantia* lectin (AAL)² from mushroom (11), *Rhizopus stolonifer* lectin from fungi (12), and *Ralstonia solanacearum* lectin from bacteria (13). Among these lectins, AAL and *R. stolonifer* lectin preferentially bind to α 1,6-fucosylated oligosaccharides, whereas *Ulex europaeus* and *Lotus tetragonolobus* lectins prefer α 1,2-linked fucose residues (14). AAL is a commercially available lectin that is known for its high affinity for α 1,6-fucosylated oligosaccharides (15), and it is widely used to estimate the

* The costs of publication of this article were defrayed in part by the payment of page charges. This article must therefore be hereby marked "advertisement" in accordance with 18 U.S.C. Section 1734 solely to indicate this fact.

[‡] The on-line version of this article (available at <http://www.jbc.org>) contains supplemental Fig. S1.

¹ To whom correspondence should be addressed: Research Institute, Gekkeikan Sake Co. Ltd., 300 Katahara-cho, Fushimi-ku, Kyoto 612-8361, Japan. Tel.: 81-75-623-2104; Fax: 81-75-623-2455; E-mail: kengo@gekkeikan.co.jp.

² The abbreviations used are: AAL, *Aleuria aurantia* lectin; LCA, *Lens culinaris* agglutinin; AOL, *Aspergillus oryzae* lectin; PA, pyridylaminated; SPR, surface plasmon resonance; FGP, α 1,6-fucosylated glycopeptide; MEF, mouse embryo fibroblasts; FUT8, α 1,6-fucosyltransferase; SGP, sialylglycopeptide; PBS, phosphate-buffered saline; RU, resonance units; GlcNAc, N-acetylglucosamine; MES, 4-morpholineethanesulfonic acid.

extent of α 1,6-fucosylation (core fucosylation) on glycoproteins and to fractionate glycoproteins (16). Another lectin that recognizes oligosaccharides containing core fucose would be a valuable tool in glycobiological research because only a few lectins have been identified as specific for core fucose, and AAL itself exhibits broad specificity for α 1,2-, α 1,3-, and α 1,4-fucose-containing oligosaccharides (17).

We previously identified a novel lectin, AOL, in iron-deficient cultures of the filamentous fungus *A. oryzae*; this lectin turned out to be L-fucose-specific from a hemagglutination inhibition assay using several monosaccharides and the encoding gene, *fleA*, was found to share 26% homology with AAL in primary structure (18). Here, to verify whether AOL might be a valuable tool in glycobiological studies involving immunochemical, biochemical, and functional techniques for characterizing, we have examined the carbohydrate binding specificity of AOL by using SPR analysis, lectin affinity chromatography, lectin blot analysis, and immunocytochemical staining as compared with AAL. Our results indicate that AOL is, to our knowledge, the most specific probe for core fucose identified so far.

EXPERIMENTAL PROCEDURES

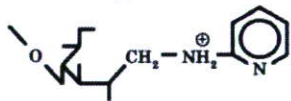
Materials—AAL and LCA were purchased from Seikagaku Kogyo (Tokyo, Japan). The seven PA-sugar chains were purchased from Takara Bio. (Kyoto, Japan). The Lewis x trisaccharide was purchased from Dextra Laboratories, Ltd. (Reading, UK). The nonlabeled sugar was pyridylaminated with GlycoTag (Takara Bio) and then was subjected to a Cellulose Cartridge Glycan preparation kit (Takara Bio) to obtain α 1,3-fucosylated (tri Le-x) PA-sugar chain. Structures of the differently fucosylated oligosaccharides used are shown in Table 1 and Fig. 6. Neuraminidase, β -galactosidase, and α 1,6-fucosyltransferase were purchased from Nakarai Tesque (Kyoto, Japan), Seikagaku Kogyo and TOYOBO (Osaka, Japan), respectively.

Preparation of FGP—FGP was prepared from a sialylglycopeptide (SGP) obtained from egg yolk as described by Seko *et al.* (19). In brief, the SGP (2.5 mg) was dissolved in 0.2 ml of 50 mM sodium citrate buffer, pH 5.0, and incubated with neuraminidase (3 units) at 37 °C for 24 h. The mixture was heated in a boiling water bath for 5 min and centrifuged at 10,000 \times g, and then the supernatant was subjected to a Cellulose Cartridge Glycan preparation kit (Takara Bio) to obtain the asialo-glycopeptide. This asialo-glycopeptide (1.28 mg) was dissolved in 200 μ l of 50 mM sodium citrate buffer, pH 5.0, and digested with β -galactosidase (5 units) at 37 °C for 48 h. After purification with the Cellulose Cartridge, the glycopeptide was dissolved in 0.2 ml of 200 mM MES buffer, pH 7.0, and then incubated with α 1,6-fucosyltransferase (5 mU) at 37 °C for 24 h. The products were fluorescently labeled with *N*-[2-(2-pyridylamino)ethyl] succinamic acid 5-norbornene-2,3-dicarboximide ester (WAKO) and purified by HPLC as described previously (20). The structure of the FGP was confirmed by matrix-assisted laser desorption/ionization time-of-flight mass spectrometry.

Preparation of AOL—AOL was prepared by expressing the encoding gene, *fleA*, in the homologous hyperexpression system of *A. oryzae* as we described previously (18). The *A. oryzae*

Carbohydrate Binding Specificity of *A. oryzae* Lectin

TABLE 1
Structure of PA-sugar chains and FGP

α 1,6 (N): <i>N</i> -Acetyllactosamine type, tetraantennary	$\begin{array}{c} \text{Gal}\beta(1-4)\text{GlcNAc}\beta(1-6) \\ \text{Gal}\beta(1-4)\text{GlcNAc}\beta(1-2)\text{Man}\alpha(1-6) \\ \text{Gal}\beta(1-4)\text{GlcNAc}\beta(1-2)\text{Man}\alpha(1-3) \\ \text{Gal}\beta(1-4)\text{GlcNAc}\beta(1-4) \end{array} \text{Man}\beta(1-4)\text{GlcNAc}\beta(1-4)\text{GlcNAc-PA} \text{Fuca}(1-6)$
α 1,3 (N): <i>N</i> -Acetyllactosamine type, tetraantennary	$\begin{array}{c} \text{Gal}\beta(1-4)\text{GlcNAc}\beta(1-6) \\ \text{Gal}\beta(1-4)\text{GlcNAc}\beta(1-2)\text{Man}\alpha(1-6) \\ \text{Gal}\beta(1-4)\text{GlcNAc}\beta(1-2)\text{Man}\alpha(1-3) \\ \text{Gal}\beta(1-4)\text{GlcNAc}\beta(1-4) \\ \text{Fuca}(1-3) \end{array} \text{Man}\beta(1-4)\text{GlcNAc}\beta(1-4)\text{GlcNAc-PA}$
α 1,2 (H antigen): Lacto- <i>N</i> -fucopentaose I	Fuca(1-2)Gal β (1-3)GlcNAc β (1-3)Gal β (1-4)Glc-PA
α 1,4 (O) Lewis A: Lacto- <i>N</i> -fucopentaose II	Gal β (1-3)GlcNAc β (1-3)Gal β (1-4)Glc-PA Fuca(1-4)
α 1,3 (O) Lewis X: Lacto- <i>N</i> -fucopentaose III	Gal β (1-4)GlcNAc β (1-3)Gal β (1-4)Glc-PA Fuca(1-3)
α 1,2 (A antigen): A-hexasaccharide	GalNAc α (1-3)Gal β (1-3)GlcNAc β (1-3)Gal β (1-4)Glc-PA Fuca(1-2)
Fucosylglycopeptide (FGP)	$\begin{array}{c} \text{GlcNAc}\beta(1-2)\text{Man}\alpha(1-6) \\ \text{GlcNAc}\beta(1-2)\text{Man}\alpha(1-3) \end{array} \text{Man}\beta(1-4)\text{GlcNAc}\beta(1-4)\text{GlcNAc}\beta(1-4)\text{GlcNAc}\beta(1-4)\text{GlcNAc-PA} \text{Fuca}(1-6) \text{Lys} \text{Ala} \text{Asn} \text{Lys} \text{Thr} \text{Val}$
Fuc, fucose; Man, mannose; Gal, galactose; GlcNAc, <i>N</i> -acetylglucosamine. GlcNAc-PA (Pyridylaminated GlcNAc); 	

mycelium was used to prepare intracellular protein. A transformant harboring the *fleA* gene under the control of the *melO* promoter was cultured in 100 ml of modified Czapek-Dox medium (0.3% NaNO₃, 0.2% KCl, 0.1% KH₂PO₄, 0.05% MgSO₄·7H₂O, 0.002% FeSO₄·7H₂O together with 6% glucose, pH 6.0) at 30 °C for 7 days. After collecting the mycelia, a cell-free extract was prepared by disruption with sea sand in 20 mM sodium phosphate buffer (pH 7.0) containing 1.0 mM phenylmethylsulfonyl fluoride. The resultant homogenate was centrifuged (10,000 \times g, 10 min), and the supernatant was used for further purification.

All purification steps were performed at 4 °C. After salt precipitation with ammonium sulfate, the active hemagglutinating fraction (precipitated at 0.30–0.75 saturation) of the cell-free extract was suspended in 20 mM sodium phosphate buffer (pH 6.0). The suspension was dialyzed overnight against the same buffer and then applied to a column of CM Toyoperl 650 M, 1.6 cm \times 10 cm (TOSO, Tokyo, Japan), equilibrated with 50 mM sodium phosphate buffer (pH 6.0). AOL was eluted with a 0–500 mM NaCl linear gradient in the same buffer. The peak fractions with hemagglutinating activity were pooled and dialyzed overnight against the same buffer. Purified AOL was stored at 4 °C because freezing causes 15–20% loss of the protein.

Carbohydrate Binding Specificity of *A. oryzae* Lectin

SPR Measurements—The Biacore 2000 instrument, BIA evaluation software 3.0, sensor chip CM5 and the amino coupling kit were obtained from Biacore AB (Uppsala, Sweden). The surface of a research grade CM5 sensor chip was activated at a flow rate of 5 $\mu\text{l}/\text{min}$ with 1:1 mixture of *N*-hydroxysuccinimide and *N*-ethyl-*N'*-(dimethylaminopropyl) carbodiimide solution for 20 min. Each lectin, at a concentration of 100 $\mu\text{g}/\text{ml}$ in 10 mM sodium acetate buffer, pH 5.0, was injected for 20 min, and the remaining *N*-hydroxysuccinimide esters were blocked by the addition of 1 M ethanolamine, for 20 min. AOL, AAL, and LCA were immobilized to flow cells on the CM5 sensor chip at 322, 413, and 541 fmol, respectively. Measurements were carried out simultaneously on all four measuring channels of which three were immobilized AOL, AAL, and LCA, and the fourth channel was the reference flow cell. The fourth channel was treated identically except for the injection of lectin. All analyses were performed at 25 °C in HBS buffer (10 mM Hepes buffer, pH 7.4 containing 0.01% Tween 20) at a flow rate of 50 $\mu\text{l}/\text{min}$. The concentrations of PA-sugar chains and FGP solutions were, respectively, 1.0 and 7.0 nmol/ml in 100 μl of HBS buffer. The analytes were injected for 2 min, and after a dissociation period of 3.5 min, the surface was regenerated with a 1-min pulse of 100 mM glycine buffer, pH 3.0. All binding experiments were repeated three times, and similar results were obtained.

Fractionation of PA-Sugar Chains by AOL or AAL Lectin Affinity Chromatography—Purified AOL (2.5 mg) and AAL (2.7 mg) were each dissolved in 200 mM sodium acid carbonate buffer (pH 8.3) containing 0.5 M NaCl and coupled to an NHS-activated HiTrap column (1 ml; GE Healthcare, Buckinghamshire, UK) according to the manufacturer's instructions. The amount of protein immobilized was determined by measuring the amount of uncoupled protein in the wash fraction. Lectin affinity chromatography was performed at room temperature. The AOL- or AAL-immobilized column was equilibrated with 50 mM sodium phosphate buffer (pH 7.4), containing 0.15 M NaCl. α 1,6-fucosylated (biantennary), and α 1,3-fucosylated (tri Le-x) PA-sugar chains (80 μmol each) were applied to each column. The non-bound fraction was eluted with four volumes of equilibration buffer. The bound fraction was eluted with a linear gradient of 0.05–0.55 mM fucose in equilibration buffer applied over five volumes, and the column was then washed with a volume of 1 mM fucose, a volume of 10 mM fucose, and four volumes of equilibration buffer. Fractions of 0.5 ml were collected throughout. To separate PA-sugar chains, a 20- μl aliquot of each fraction was applied to reversed-phase HPLC using 20 mM phosphate buffer, pH 4.0, containing 1.0% (v/v) *n*BtOH, at 40 °C. Each PA-sugar chain was quantified by fluorescence.

Biotinylation of Lectins—AOL, AAL, and LCA were biotinylated using a biotin labeling kit from Roche Applied Science (Tokyo, Japan). The *D*-biotinoyl- ϵ -aminocaproic acid-*N*-hydroxysuccinimide ester (15 μl ; 2 mg/ml in dimethylformamide) was added dropwise to a solution of each lectin (1.0 ml; 1.0 mg/ml in phosphate-buffered saline (PBS)) while being agitated with a vortex mixer. After incubation for 2 h at room temperature with gentle stirring, the labeled lectin was collected by

Sephadex G-25 column chromatography and stored at 4 °C until use.

Lectin Blot Analysis—Lectin blot analyses were performed as described previously (21). In brief, 10 μg of protein was subjected to 8% SDS-PAGE. After electrophoresis, the gels were blotted onto nitrocellulose membranes. The membranes were incubated overnight with 3% bovine serum albumin in Tris-buffered saline (20 mM Tris, 0.5 M NaCl, pH 7.5; TBS), and then for 1 h with 1.9 $\mu\text{g}/\text{ml}$ of biotinylated AOL lectins or 0.5 $\mu\text{g}/\text{ml}$ of biotinylated AAL in TBST (TBS containing 0.05% Tween 20). After being washed with TBST, the membranes were incubated with horseradish peroxidase-conjugated avidin (VECTASTAIN ABC kit; Vector Laboratories, Burlingame, CA) for 30 min and then washed with TBST. Staining was performed with ECL Western blot detection reagents (GE Healthcare).

Cytochemical Staining with Lectins—MEF cell cultures were prepared as previously described (22). In brief, cultures of fibroblasts from wild-type or Fut8 knock-out mice (22) were prepared by trypsinization of 14–15 day embryos. The cells were grown in Dulbecco's modified Eagle's medium (Sigma) at 37 °C in a humidified incubator supplied with 5% CO₂ in air. The cell solution (0.3 ml) was plated at an initial density of 1.0×10^4 cells/ml on coverslips (Fisher Scientific Waltham, MA), and placed in current 24-well cell-culture plates (IWAKI Chiba Japan). The cells were incubated for 24 h before examination and were washed three times with PBS buffer at 0.5 ml/well (washing step). The cells were fixed in 0.1 M phosphate buffer containing 4% paraformaldehyde for 20 min at room temperature and dehydrated in ice-cold ethanol for 10 min after the washing step. Unbound sites were blocked by incubation with 200 μl of 1.0% (w/v) bovine serum albumin in washing solution for 30 min. After the blocking solution was removed, the wells were incubated with 100 μl of biotinylated AOL (5.0 or 50 $\mu\text{g}/\text{ml}$) or AAL (2.5 or 5.0 $\mu\text{g}/\text{ml}$) in blocking solution for 2 h at room temperature. Localization of lectin was visualized by an avidin-biotin coupling immunofluorescence technique. The cultured cells were incubated with streptavidin, Alexa Fluor 546 conjugate (Molecular Probes S11225, Eugene, OR) at room temperature for 1 h, then washed and mounted with aqueous mounting medium (Permaflour, Beckman-Coulter, Paris, France). Fluorescent images were analyzed with an Olympus fluorescence microscope BXF50–3 (Olympus, Tokyo, Japan).

RESULTS

Preparation and Protein Characteristics of AOL—To clarify the function of AOL, its encoding gene *fleA* was overexpressed in *A. oryzae*, resulting in a maximum yield of 1.0 g/liter-broth/7 d of AOL. The intracellular recombinant AOL was purified to such an extent that it resulted in the agglutination of rabbit red blood cells at a concentration of 3.9 $\mu\text{g}/\text{ml}$ of lectin in PBS (pH 7.2), as described under "Experimental Procedures." The purified AOL gave a single band on SDS-PAGE (Fig. 1 lane 1).

As we described previously, AOL shares 26% homology with AAL in primary structure (18). As shown in Fig. 1, the molecular weight of AOL on SDS-PAGE was 35,000, a little higher than that of AAL. By contrast, LCA appeared as two bands corresponding to molecular weights of 6000 and 18,000. Previous studies have reported the molecular weight of AAL as 66,796,

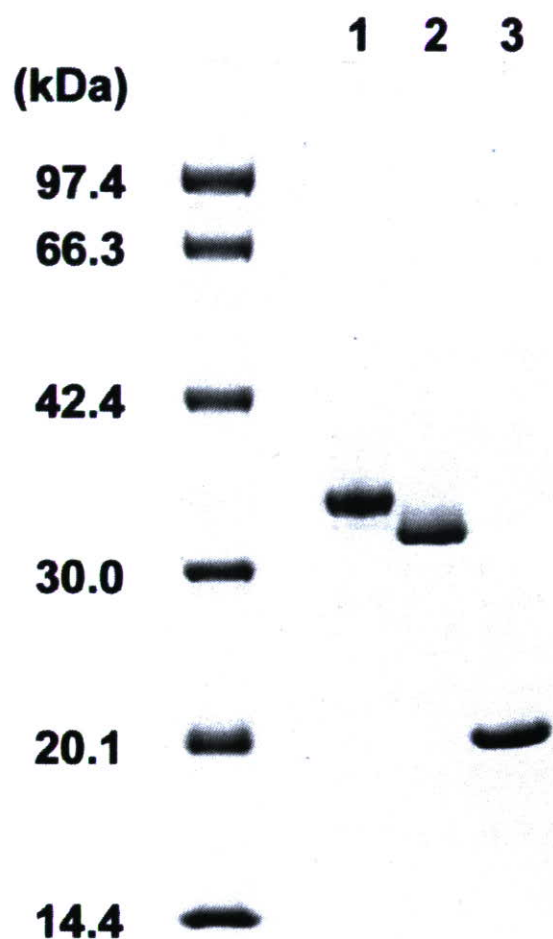


FIGURE 1. SDS-PAGE analysis of AOL compared with AAL and LCA. Electrophoresis was done by the method of Laemmli (23) on a 10–20% gradient polyacrylamide gel (Daiichi Chemicals, Tokyo, Japan) in buffer comprising 25 mM Tris-HCl, 0.192 M glycine and 0.1% SDS. The gel was stained with Coomassie Brilliant Blue R-250. Approximately 1 μ g of protein was run in each lane. Lane 1, AOL; lane 2, AAL; lane 3, LCA.

consisting of identical subunits of 33,398 (15), and that of LCA as 46,000, consisting of four subunits ($\alpha_2\beta_2$): two of 5,710 and two of 17,572 (24). In SPR analysis, HCl injection (100 mM, 100 μ l) into a CM5 sensor chip flow cell immobilized with purified AOL resulted in a decrease in resonance units (RU), corresponding to approximately half the amount of immobilized ligand (data not shown), which suggests that AOL consists of two identical subunits. In addition to the three-dimensional structure, AOL and AAL were found to have almost the same isoelectric point, pI 9.0 (data not shown). These results suggest that AOL is similar to AAL not only in amino acid sequence but also in protein characteristics.

The Carbohydrate Binding Specificity of AOL—An oligosaccharide binding study has shown that AAL is highly specific for α 1,6-fucosylated oligosaccharides (16). To elucidate whether AOL is equally specific for α 1,6-fucosylated oligosaccharides, we investigated the interaction of six differently fucosylated PA-sugar chains with AOL immobilized to a CM5 sensor chip

Carbohydrate Binding Specificity of *A. oryzae* Lectin

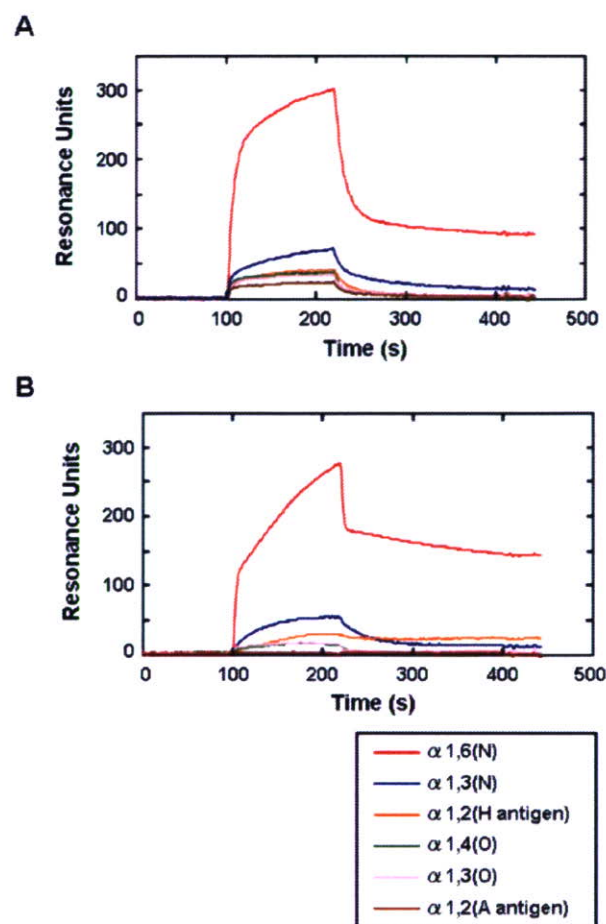


FIGURE 2. Overlay plot of sensorgrams showing the interaction of PA-sugar chains with immobilized AOL or AAL. Solutions of six different PA-sugar chains were injected over an AOL (A) or AAL (B) surface. AOL and AAL were immobilized on the surface of flow cells of a CM5 sensor chip at 322 and 413 fmol, respectively. The structures of the six differently fucosylated PA-sugar chains are shown in Table 1. All analyses were performed at 25 °C using HBS buffer (10 mM HEPES buffer, pH 7.4 containing 0.01% Tween 20) and a flow rate of 50 μ l/min. The PA-sugar chain solutions (1 nmol/ml) were injected for 2 min, and after a dissociation of 3.5 min the surface was regenerated with a 1-min pulse of 100 mM glycine buffer, pH 3.0. The binding curves for all analytes were deduced after subtracting the response of the reference surface.

flow cell. The molar amount of each PA-sugar chain that interacts with AOL can be deduced from the differences in the RU values of an overlay plot of the sensorgrams (Fig. 2A), which are equivalent to mass change. From the molar amount of each PA-sugar chain that interacted with immobilized AOL (Fig. 3A, solid bar), AOL has the strongest preference for the α 1,6-fucosylated PA-sugar chain among the α 1,2-, α 1,3-, α 1,4-, and α 1,6-fucosylated chains tested. These results suggest that, like AAL, AOL is highly specific for α 1,6-fucosylated oligosaccharides.

Comparison of the Carbohydrate Binding Specificity of AOL, AAL, and LCA—AAL and LCA are widely used to estimate the extent of core fucosylation on glycoproteins and to fractionate glycoproteins. To compare the carbohydrate binding specificity of AOL with that of AAL and LCA, we investigated the interaction of the six PA-sugar chains with these lectins immobilized to the CM5 sensor chip flow cells by using BIAcore. As shown in Fig. 2, AOL and AAL showed binding to the PA-sugar chains

Carbohydrate Binding Specificity of *A. oryzae* Lectin

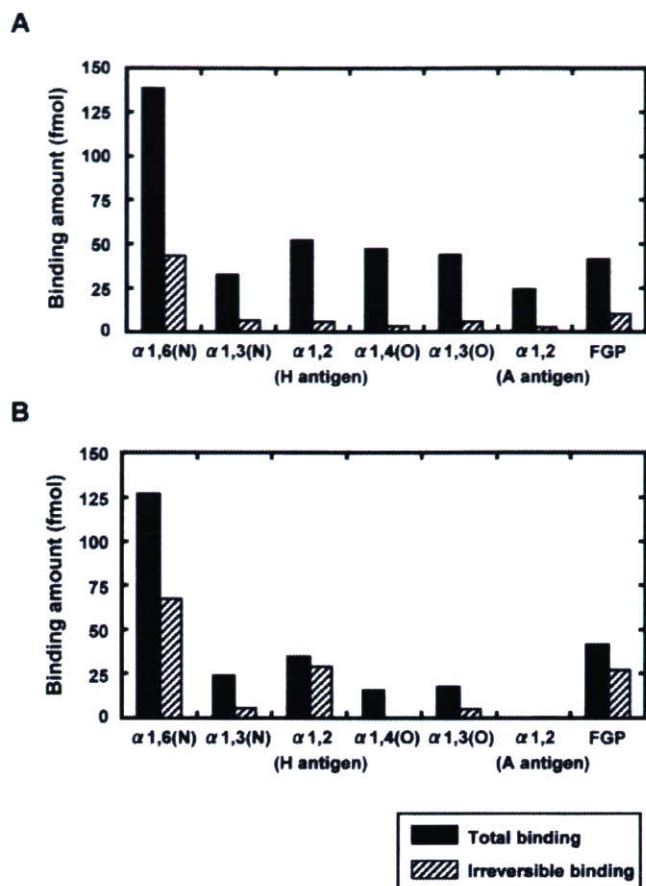


FIGURE 3. The molar amount of each PA-sugar chain that interacts with AOL or AAL. The molar amount of each PA-sugar chain that interacts with AOL (A) or AAL (B) was deduced from the differences in the RU values of an overlay plot of the sensorgrams (Figs. 2 and 4), which are equivalent to mass change. Total binding (solid bar) indicates differences in the 10-s average RU values before the start of injection (90–100 s) and before the end of injection (210–220 s); irreversible binding (slashed bar) indicates differences before the start of injection (90–100 s) and at equilibrium after the injection had stopped and had been replaced by a buffer flow (420–430 s).

tested, whereas LCA showed no binding to them (data not shown). From the molar amount of each PA-sugar chain that interacted with each immobilized lectin (Fig. 3, solid bar), both AOL and AAL apparently displayed similar specificities for the $\alpha 1,6$ -fucosylated PA-sugar chain. As shown in the overlay plot of sensorgrams (Fig. 2B), however, the rate of the rise in the RU value over the injection time (100–220 s) and the fall over the dissociation time (220–430 s) indicated that the binding to AAL occurs in a biphasic fashion in a series of fast and slow interactions, unlike the binding to AOL (Fig. 2A). Furthermore, the RU value at equilibrium during the dissociation time (420–430 s) in the overlay plot of sensorgrams (Fig. 2) indicated that, respectively, 1.5 times and 5.1 times as many $\alpha 1,6$ (N) and $\alpha 1,2$ (H antigen) fucosylated PA-sugar chains remained bound to AAL without dissociation as remained bound to AOL. These results suggest that the irreversible binding of these PA-sugar chains is much stronger to AAL than to AOL. Consequently, we compared the carbohydrate-binding specificity of AOL with that of AAL for two different binding properties: namely, total

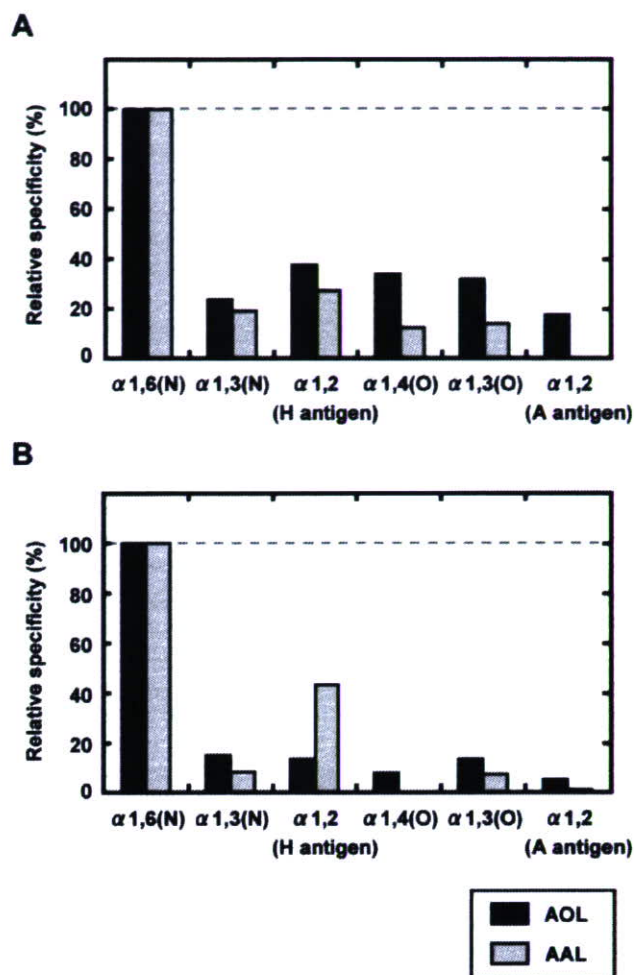


FIGURE 4. Comparison of the specificity of AOL and AAL for core fucosylation. The molar amount of the fucosylated PA-sugar chains binding to AOL (black bar) or AAL (gray bar) relative to that of $\alpha 1,6(N)$ PA-sugar chain was deduced from the molar amount of each PA-sugar chain that interacts with AOL or AAL (Fig. 3). Total binding (A); irreversible binding (B). Results are shown as a percentage of the molar amount of $\alpha 1,6$ -fucosylated PA-sugar chain (taken to be 100%) that interacted with each lectin (mol/mol).

binding and irreversible binding, as shown in Fig. 3 (solid bar and slashed bar, respectively).

Comparison of Specificity for Core Fucosylation of AOL with That of AAL—To elucidate which is the more specific lectin for core fucosylation, we determined whether AOL or AAL showed quantitatively lower binding to the other fucosylated PA-sugar chains relative to $\alpha 1,6$ -fucosylated PA-sugar chains. From the results of total binding shown in Fig. 4A, AAL displayed quantitatively lower binding to other fucosyl PA-sugar chains relative to the $\alpha 1,6$ -fucosylated PA-sugar chain than did AOL. From the results of the irreversible binding shown in Fig. 4B, however, the amount of AAL binding to $\alpha 1,2$ (H antigen) relative to $\alpha 1,6$ (N) PA-sugar chains is higher than that of AOL. Taken together, we conclude that AOL is more specific for core fucosylation than is AAL in terms of irreversible binding.

Comparison of the Specificity of AOL for FGP with That of AAL and LCA—As described above, we investigated the interactions of lectins with PA-sugar chains to determine their spec-

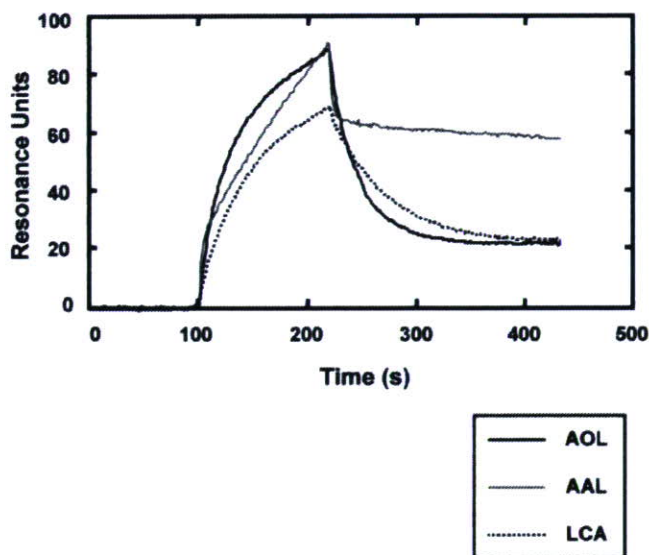


FIGURE 5. Overlay plot of sensorgrams of the interaction of FGP with immobilized AOL or AAL. A solution of FGP was injected over an AOL, AAL, or LCA surface. AOL, AAL, and LCA were immobilized to the surface of to flow cells of a CM5 sensor chip at 322, 413, and 414 fmol, respectively. The structure of FGP is shown in Table 1. All analyses were performed at 25 °C in HBS buffer (10 mM Hepes buffer, pH 7.4 containing 0.01% Tween 20) and a flow rate of 50 μ l/min. The FGP solution (7 nmol/ml) was injected for 2 min, and after a dissociation of 3.5 min the surface was regenerated with a 1-min pulse of 100 mM glycine buffer, pH 3.0.

ificities for fucosylated oligosaccharides. However, PA-sugar chains are artificial oligosaccharides and may not be representative of *in vivo* fucosylated oligosaccharides owing to the decyclization of the reducing terminal *N*-acetylglucosamine (GlcNAc) of these sugar chains with pyridylamine (Table 1). Then, to compare the interactions of the lectins with an oligosaccharide of *in vivo* glycoproteins, we purified FGP from hen's egg yolk as described under "Experimental Procedures." FGP has *N*-glycans with α 1,6-fucosyl residue bound to the core GlcNAc linked to peptide as shown in Table 1. The linked peptide chain has three amino groups (two lysine residues and the *N*-terminal group) and, after fluorescent labeling, an average of 2.0 of these three amino groups were labeled with *N*-[2-(2-pyridylamino)ethyl]succinamic acid 5-norbornene-2,3-dicarboxyimide ester (data not shown). As shown in Fig. 5, the rate of the rise in the RU value over the injection time (100–220 s) and the rate of the fall over the dissociation time (220–430 s) indicated that binding to AAL occurs in a biphasic fashion in a series of fast and slow interactions, and the RU value at equilibrium during the dissociation time (420–430 s) indicated that 2.6 times as much FGP remains bound to AAL without dissociation as remains bound to AOL. These results were similar to the plots for binding to the α 1,6 (N) PA-sugar chains shown in Fig. 2. From the irreversible binding (Fig. 3, *slashed bar*), however, the interactions of FGP with immobilized AOL and AAL were weaker than those of the α 1,6 (N) PA-sugar chains, respectively. This weaker binding must result from a stronger electrostatic repulsion from FGP than from the PA-sugar chains because both AOL and AAL have positive charges under the conditions used for SPR analysis at pH 7.4 and FGP has more positive charges than the PA-sugar chains. In addition,

Carbohydrate Binding Specificity of *A. oryzae* Lectin

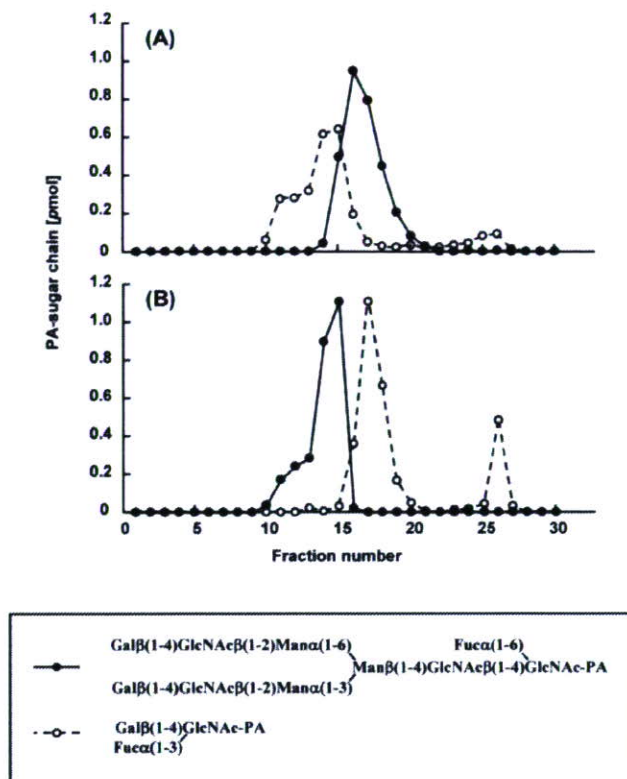


FIGURE 6. Comparison of fractionation of fucosylated oligosaccharides by AOL and AAL lectin affinity chromatography. α 1,6-fucosylated (biantennary) and α 1,3-fucosylated (tri Le-x) PA-sugar chains were applied to an AOL (A) or AAL (B)-immobilized column (bed volume, 1 ml) equilibrated with 50 mM sodium phosphate buffer, pH 7.4, containing 0.15 M NaCl, at room temperature. Fractions of 0.5 ml were collected throughout, and each PA-sugar chain was separated by reversed-phase HPLC and quantified by fluorescence. Initially, four volumes of equilibration buffer were applied to elute the non-bound fraction, and then a linear gradient of 0.05–0.55 mM fucose in the same buffer was applied over five volumes, followed by a volume of 1 mM fucose, a volume of 10 mM fucose, and four volumes of equilibration buffer. *Closed circles*, α 1,6-fucosylated (biantennary); *open circles*, α 1,3-fucosylated (tri Le-x) PA-sugar chains.

unlike the PA-sugar chains, FGP showed binding to LCA (Fig. 5). The lack of interaction between LCA and the PA-sugar chains results from decyclization of the reducing terminal GlcNAc with pyridylamine. Taken together, these results suggest that AOL and AAL bind to FGP in the same manner as they bind to the α 1,6 (N) PA-sugar chains whether or not the oligosaccharides have decyclization of the reducing terminal GlcNAc.

Comparison of Fractionation of Fucosylated Oligosaccharides by AOL Lectin Affinity Chromatography with That by AAL—To test the specificity of AOL for core fucose in other applications, we compared the fractionation of α 1,6-fucosylated (biantennary) and α 1,3-fucosylated (tri Le-x) PA-sugar chains using an AOL-immobilized column with that using an AAL-immobilized column. The PA-sugar chains were applied to each column as described under "Experimental Procedures," and neither chain was detected in the flow-through fraction of the respective columns. The PA-sugar chains that bound to the immobilized lectins were eluted with fucose as a competitive binding substance. When the bound fraction was eluted with 10

Carbohydrate Binding Specificity of *A. oryzae* Lectin

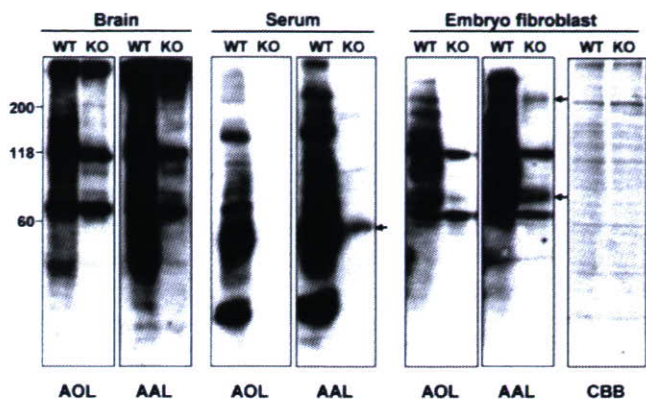


FIGURE 7. Comparison of the proteins in wild-type and *Fut8* knock-out mice by AOL- and AAL-lectin blot analyses. 10 μg of proteins from brain, serum and MEF of wild-type (WT) and *Fut8* knock-out (KO) mice were subjected to 8% SDS-PAGE, followed by AOL- and AAL-lectin blot analyses; Coomassie Brilliant Blue staining was also carried out on the same samples. In the glycoproteins from *Fut8* knock-out mice, the bands that showed enhanced intensity in the AAL blot analysis as compared with the AOL blot analysis are indicated by an arrow. See "Experimental Procedures" for full details.

mm fucose, both PA-sugar chains eluted in more or less the same fraction and could not be separated by the lectins (data not shown). Because AAL has millimolar range affinity ($K_d = 1.6 \times 10^{-4}$ M) for fucose (11), we next eluted the bound fraction with a linear gradient of 0.05–0.55 mM fucose (applied over five volumes of equilibrium buffer), which is near the K_d value for AAL binding of fucose. As shown in Fig. 6, α 1,6-fucosylated PA-sugar chains bound to the AOL column showed a delay in elution peak as compared with those bound to the AAL column. In contrast, α 1,3-fucosylated PA-sugar chains bound to the AOL column eluted earlier than those bound to the AAL column. As a result, an opposing elution order of PA-sugar chains (cross-over) was obtained from these two lectin columns. Furthermore, fraction No. 26 from the AAL column, eluted by 10 mM fucose, contained more α 1,3-fucosylated PA-sugar chain than did fraction No. 26 from the AOL column, suggesting that AAL shows stronger interaction with part of the bound α 1,3-fucosylated PA-sugar chain than AOL. Taken together, these results show that AOL has higher specificity for core fucose than AAL.

Comparison of Lectin Blot Analysis by AOL and AAL—To test the possibility that AOL might be a valuable tool in glyco-biological studies, we carried out lectin blot analysis of glycoproteins from the brain, serum and MEF of wild-type and *Fut8* knock-out mice using biotinylated AOL or AAL. As shown in Fig. 7, the pattern of brain glycoproteins was very similar between the AOL and AAL blot analyses, with the exception that the intensity of AAL binding was slightly higher than that of AOL binding. For the serum and MEF glycoproteins from *Fut8* knock-out mice, however, the bands, which are indicated by an arrow showed enhanced intensity in the AAL blot analysis as compared with the AOL blot analysis. The staining for bands at 118 and 70 kDa, which remain in brain tissue and embryonic cells, but not serum, from *Fut8* knock-out mice appear to be nonspecific because they are also detected by the avidin-horse-radish peroxidase conjugate in the absence of lectins (data not shown). These results show that serum and MEF glycoproteins

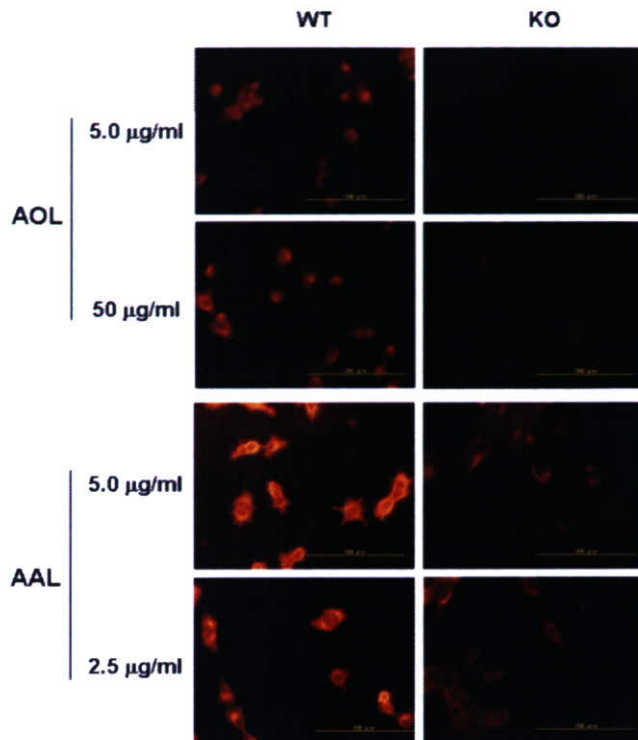


FIGURE 8. Analysis of fucosylation levels in the embryo fibroblasts of wild-type and *Fut8* knock-out mice. Cultured MEF cells obtained from wild-type or *Fut8* knock-out mice were fixed with 4% paraformaldehyde. Sample wells were pretreated by hydroxybenzotriazole blocking and then incubated with biotinylated AOL (5.0 or 50 $\mu\text{g}/\text{ml}$) or AAL (2.5 or 5.0 $\mu\text{g}/\text{ml}$) for 2 h at room temperature, followed by fluorescein staining. The orange color indicates positive lectin staining.

contain many fucose residues other than core fucose because the expression of fucosyltransferases is regulated tissue-specifically, and that AAL lectin strongly recognizes these residues as compared with AOL.

Comparison of Cytochemical Staining by AOL and AAL—As shown in Fig. 7, lectin blot analysis showed that AOL is more specific for core fucosylation than AAL, especially in MEF glycoproteins. To confirm the specificity of AOL for core fucosylation, we compared the cytochemical staining of cultured MEF cells from wild-type and *Fut8* knock-out mice using biotinylated AOL or AAL. As shown in Fig. 8, positive staining for AOL and AAL at 5 $\mu\text{g}/\text{ml}$ was clearly observed in cultured MEF cells from wild-type mice and, importantly, AOL staining, but not AAL staining, was completely abolished in cultured MEF cells from *Fut8* knock-out mice. However, the intensity of AOL staining of the cells from wild-type mice was weaker than that of AAL, and we therefore compared AOL staining at 50 $\mu\text{g}/\text{ml}$ with AAL staining at 2.5 $\mu\text{g}/\text{ml}$, respectively. Even with a 20-fold higher amount of lectin, AOL staining of cultured MEF cells from *Fut8* knock-out mice seemed to be much weaker than AAL immunostaining, further suggesting that AOL, as compared with AAL, shows quantitatively lower binding to other fucosylated oligosaccharides relative to α 1,6-fucosylated oligosaccharides. Taken together, these results show that AOL is a more specific probe for core fucose than AAL.

TABLE 2
Comparison of protein characteristics between AOL and AAL

Properties	AOL	AAL
Amino acid residues	310 ^a	312 ^b
Amino acid homology to AAL	26% ^a	100%
Subunit molecular weight	34,481	33,398 ^b
Three-dimensional structure	Homodimer	Homodimer ^c
pI	9.0	9.0
Specificity of monosaccharide	L-Fuc >> D-Man, NANA ^a	L-Fuc >> D-Ara ^b
Specificity of oligosaccharides	α Fuc1,6 >> 1,2, 1,3, 1,4	α Fuc1,6 >> 1,2, 1,3, 1,4
Binding fashion of oligosaccharides	Fast	Fast and slow
Irreversible binding of oligosaccharides	Weak	Strong
Family	Six-fold β -propeller?	Six-fold β -propeller ^d

^a Ishida *et al.* (18).^b Fukumori *et al.* (15).^c Yamashita *et al.* (16).^d Wimmerova *et al.* (17).

DISCUSSION

We have shown here that AOL is highly specific for core fucose and that the binding specificities of this lectin are more suitable for detecting core fucosylation than those of AAL and LCA.

As summarized in Table 2, AOL and AAL share similar protein characteristics. We therefore anticipated that AOL, like AAL, would show specificity for core fucose. AAL has a six-fold β -propeller structure and forms six clefts between each blade, as determined from its crystal structure by Wimmerova *et al.* (17) and Fujihashi *et al.* (25). This fold is a type that is found in lectins of soil inhabitants and it displays multivalent carbohydrate recognition that has been proposed to be involved in the host recognition strategy of several pathogenic organisms, including the phytopathogenic bacterium *R. solanacearum* (17, 26). AOL contains six sequence repeats that are highly similar to those of AAL, and it has been suggested that AOL also has a six-fold β -propeller structure (17). The specificity of AOL for core fucosylation found in this study would reflect a similarity in the structures of these two lectins.

In contrast to their similar specificity for core fucose in SPR analysis, the following two of our results suggested that AOL and AAL bind to fucosylated oligosaccharides in a different manner. First, from the plots of Figs. 2B and 5, binding of the α 1,6 (N) PA-sugar chain and FGP to AAL occurred in a biphasic fashion, unlike their binding to AOL (Figs. 2A and 5). We speculate that these biphasic interactions of AAL indicate the different affinity of the fucose-binding sites toward fucosylated oligosaccharides. Recently, the crystallographic structure of AAL has been independently determined by Wimmerova *et al.* (17) and Fujihashi *et al.* (25). In the two structures reported by these two groups, the overall protein structures look identical to each other, however, the fucose molecules are found in five of the six clefts in a monomer by Wimmerova *et al.*, but in only three by Fujihashi *et al.* According to Wimmerova *et al.*, five fucose residues are located in the binding pockets (sites 1–5) in the crystal structure of AAL-fucose complex, and there are strong similarities between the binding sites, which are made up from six repeats in the amino acid sequence of AAL. On the other hand, according to Fujihashi *et al.*, the five binding sites of AAL have different affinities for fucose: sites 2 and 4 are strong binding sites, site 1 may be medium in strength, sites 3 and 5 are relatively weak, and site 6 is not a fucose-binding site. If the five fucose-binding sites of AAL have equivalent affinity,

then the interactions could not be observed in a biphasic way. Thus, our data suggest that the binding sites of AAL have different affinities for fucose. Second, AOL showed weaker irreversible bindings to α 1,6 (N) and α 1,2 (H antigen) PA-sugar chains and FGP than AAL as shown in Fig. 3 slashed bar. We speculate that the weaker irreversible binding of AOL compared with AAL was caused from the presence of fewer fucose-binding sites available on AOL, as well as lower binding affinity for fucosylated oligosaccharides. The amino acid sequence alignment of AOL and AAL demonstrates that the glutamate of the third β -strand and the tryptophan of the last β -strand that are hydrogen-bonded to fucose in AAL are replaced in sites 4 and 5, respectively, in AOL, whereas five hydrogen bonds and two strong hydrophobic contacts are conserved in the other four sites, sites 1, 2, 3 and 6, in AOL (17). At present, it is not clear whether the characteristic binding properties of this lectin family, such as multivalent carbohydrate recognition, are reflected in the multivalent fucose binding sites.

In this report, we determined which lectin is more specific for core fucosylation by elucidating which lectins show quantitatively lower binding to other fucosylated PA-sugar chains relative to the α 1,6-fucosylated PA-sugar chain. We note, however, that a direct comparison of the equilibrium dissociation constants (K_d) of AOL and AAL is required for a clear physical interpretation of such bindings. Kinetic parameters such as the association (k_{on}) and dissociation (k_{off}) rate constants can be calculated directly from the sensorgram response (Fig. 2), which was fitted to a 1:1 steady-state affinity model by using BIA evaluation 3.0 software. In that experiment, the α 1,6 (N) PA-sugar chain was injected at various concentrations, 0.25, 0.5, 1.0, 1.5, 2.0 μ M, into a flow cell containing immobilized lectin (data not shown). The k_{on} and k_{off} values were determined to be $3.03 \times 10^4 \text{ M}^{-1} \text{ s}^{-1}$ and $1.57 \times 10^{-2} \text{ s}^{-1}$, respectively, for AOL, and $329 \text{ M}^{-1} \text{ s}^{-1}$ and $1.20 \times 10^{-3} \text{ s}^{-1}$, respectively, for AAL. These results suggest that the association and dissociation phases of AOL are more rapid than those of AAL. The equilibrium dissociation constants (K_d) of the α 1,6 (N) PA-sugar chain to AOL and AAL were calculated as $5.18 \times 10^{-7} \text{ M}$ and $3.65 \times 10^{-6} \text{ M}$, respectively. However, the constant calculated for AAL by SPR analysis was not in agreement with the value obtained by linearization methods because a concentration of PA-sugar chain of at least twice the K_d value is necessary to attain them correctly. Therefore, we could not directly compare the K_d values of even the α 1,6-fucosylated PA-sugar

Carbohydrate Binding Specificity of *A. oryzae* Lectin

chain, which showed the strongest binding to each lectin of all analytes. Furthermore, AAL shows stronger irreversible binding to PA-sugar chains than AOL. Consequently, we compared the carbohydrate-binding specificity of AOL with that of AAL across two different binding properties: namely, total binding and irreversible binding. Although the irreversible binding of AOL to core fucose is weaker than that of AAL, AOL is more specific for core fucosylation than AAL in terms of irreversible binding.

Lectin blot analysis and cytochemical staining of MEF showed that AOL is more reliable for detecting core fucosylation than AAL. In this regard, the intensity of lectin blotting or staining may relate to the molar amount of lectin that remains bound without dissociation (irreversible binding) during SPR analysis, because many washing steps are used in the blotting or staining processes, similar to the conditions of irreversible binding observed in SPR analysis. Two of our results support the above speculation. First, the affinity of AOL for fucose is weaker than that of AAL. SPR analysis showed that the irreversible binding of AOL to fucosylated oligosaccharides was weaker than that of AAL (Fig. 3). In fact, as compared with AAL, AOL at the same concentration (5.0 $\mu\text{g}/\text{ml}$) showed weaker staining in MEF cells from wild-type mice (Fig. 8). Second, as compared with AAL, AOL showed quantitatively lower binding to other fucosylated oligosaccharides relative to $\alpha 1,6$ -fucosylated PA-sugar chains. SPR analysis showed that irreversible binding of AOL to the $\alpha 1,2$ -fucosylated PA-sugar chain (H antigen) relative to the $\alpha 1,6$ -fucosylated chain was weaker than that of AAL (Fig. 4B). Indeed, as compared with AAL, AOL staining of cultured MEF cells from Fut8 knock-out mice seemed to be much weaker, even when 20-fold higher amounts of AOL were used (Fig. 8). The histochemical staining of brain and kidney from Fut8 knock-out mice by AAL lectin, was almost blocked in the presence of L-fucose of 2.0 $\mu\text{g}/\text{ml}$ (data not shown). The fucose-competition in immunostaining could explain that AAL has affinities to many fucose residues other than core fucose in terms of irreversible binding. Furthermore, in the fractionation of PA-sugar chains by lectin columns, AAL showed stronger interaction with part of the bound $\alpha 1,3$ fucosylated PA-sugar chain (tri Le-x) than AOL (Fig. 7). These results suggest that some multivalent fucose-binding sites of AAL have stronger affinity for fucosylated oligosaccharides not involving $\alpha 1,6$ -fucosylated linkages as compared with AOL. Taken together, staining with AAL identifies many fucose residues other than core fucose, whereas staining with AOL reflects the extent of core fucosylation on glycoproteins more clearly.

The filamentous fungus *A. oryzae* is a plant pathogen used to ferment rice in the production of sake because it has high levels of protein productivity. The *fleA* gene has been overexpressed in the homologous hyperexpression system of *A. oryzae* (18), yielding large amounts (1.0 g/liter-broth/7 days) of soluble and functional active AOL. In addition to its binding properties, this large productivity of AOL will enable it to be used widely as a novel probe for the detection of core fucose, as well as the analysis of its biological functions.

Acknowledgments—We thank Dr. Michiko Kato and Dr. Mitsuyoshi Ueda (Division of Applied Life Sciences, Graduate School of Agriculture, Kyoto University) for their help and suggestions and Jun Wada (Division of Integrated Life Science, Graduate School of Biostudies, Kyoto University) for technical advice for SPR analysis.

REFERENCES

- Drickamer, K., and Taylor, M. E. (1993) *Annu. Rev. Cell Biol.* **9**, 237–264
- Vijayan, M., and Chandra, N. (1999) *Curr. Opin. Struct. Biol.* **9**, 707–714
- Pereira, M. E. A., and Kabat, E. A. (1974) *Biochemistry* **13**, 3184–3192
- Stelck, S., Robitzki, A., Willbold, E., and Layer, P. G. (1999) *Glycobiology* **9**, 1171–1179
- Kolanus, W., Bevilacqua, M., and Seed, B. (1990) *Science* **250**, 1132–1135
- Noda, K., Miyoshi, E., Gu, J., Gao, C., Nakahara, S., Kitada, T., Honke, K., Suzuki, K., Yoshihara, H., Yoshikawa, K., Kawano, K., Tonetti, M., Kasahara, A., Hori, M., Hayashi, N., and Taniguchi, N. (2003) *Cancer Res.* **63**, 6282–6289
- Hutchinson, W. L., Du, M. Q., Johnson, P. J., and Williams, R. (1991) *Hepatology* **13**, 683–688
- Ohno, M., Nishikawa, A., Kouketsu, M., Taga, H., Endo, Y., Hada, T., Higashino, K., and Taniguchi, N. (1992) *Int. J. Cancer* **51**, 315–317
- Matsumoto, I., and Osawa, T. (1969) *Biochim. Biophys. Acta* **194**, 180–189
- Watkins, W. M., and Morgan, W. T. J. (1952) *Nature* **169**, 825–826
- Kochibe, N., and Furukawa, K. (1980) *Biochemistry* **19**, 2841–2846
- Oda, Y., Senaha, T., Matsuno, Y., Nakajima, K., Naka, R., Kinoshita, M., Honda, E., Furuta, I., and Takechi, K. (2003) *J. Biol. Chem.* **278**, 32439–32447
- Sudakevitz, D., Imberty, A., and Gilboa-Garber, N. (2002) *J. Biochem. (Tokyo)* **132**, 353–358
- Stephan, E. B., Juergen, T., Young-Ok, P., Franz-George, H., Jacques, B., and Robert, F. (1996) *Glycoconj. J.* **13**, 585–590
- Fukumori, F., Takeuchi, N., Hagiwara, T., Ohbayashi, H., Endo, T., Kochibe, N., Nagata, Y., and Kobata, A. (1990) *J. Biochem.* **107**, 190–196
- Yamashita, K., Kochibe, N., Ohkura, T., Ueda, I., and Kobata, A. (1985) *J. Biol. Chem.* **260**, 4688–4693
- Wimmerova, M., Mitchell, E., Sanchez, J. F., Gautier, C., and Imberty, A. (2003) *J. Biol. Chem.* **278**, 27059–27067
- Ishida, H., Moritani, T., Hata, Y., Kawato, A., Suginami, K., Abe, Y., and Imayasu, S. (2002) *Biosci. Biotechnol. Biochem.* **66**, 1002–1008
- Seko, A., Koketsu, M., Nishizono, M., Enoki, Y., Ibrahim, H. R., Juneja, L. R., Kim, M., and Yamamoto, T. (1997) *Biochim. Biophys. Acta* **1335**, 23–32
- Inamori, K., Endo, T., Gu, J., Matsuo, I., Ito, Y., Fujii, S., Iwasaki, H., Narimatsu, H., Miyoshi, E., Honke, K., and Taniguchi, N. (2004) *J. Biol. Chem.* **279**, 2337–2340
- Miyoshi, E., Ihara, Y., Hayashi, N., Fusamoto, H., Kamada, T., and Taniguchi, N. (1995) *J. Biol. Chem.* **270**, 28311–28315
- Wang, X., Inoue, S., Gu, J., Miyoshi, E., Noda, K., Li, W., Mizuno-Horikawa, Y., Nakano, M., Asahi, M., Takahashi, M., Uozumi, N., Ihara, S., Lee, S. H., Ikeda, Y., Yamaguchi, Y., Aze, Y., Tomiyama, Y., Fujii, J., Suzuki, K., Kondo, A., Shapiro, S. D., Lopez-Otin, C., Kuwaki, T., Okabe, M., Honke, K., and Taniguchi, N. (2005) *Proc. Natl. Acad. Sci.* **102**, 15791–15796
- Laemmli, U. K. (1970) *Nature* **227**, 680–685
- Toyoshima, S., Osawa, T., and Tonomura, A. (1970) *Biochim. Biophys. Acta* **221**, 514–521
- Fujihashi, M., Peapus, D. H., Kamiya, N., Nagata, Y., and Miki, K. (2003) *Biochemistry* **42**, 11093–11099
- Kostlanova, N., Mitchell, E., Lortat-Jacob, H., Oscarson, S., Lahmann, M., Gilboa-Garber, N., Chambat, G., Wimmerova, M., and Imberty, A. (2005) *J. Biol. Chem.* **280**, 27839–27849

A high expression of GDP-fucose transporter in hepatocellular carcinoma is a key factor for increases in fucosylation

Kenta Moriwaki², Katsuhisa Noda^{3,6}, Takatoshi Nakagawa⁴, Michio Asahi⁵, Harumasa Yoshihara³, Naoyuki Taniguchi⁷, Norio Hayashi⁶, and Eiji Miyoshi^{1,2}

²Department of Molecular Biochemistry & Clinical Investigation, Osaka University Graduate School of Medicine, 1-7, Yamada-oka, Suita, Osaka 565-0871, Japan; ³Osaka Rosai Hospital, 1179-3, Nagasone-cho, Kita-ku, Sakai, Osaka 591-8025, Japan; ⁴Departments of Glycotherapeutics; ⁵Biochemistry; ⁶Gastroenterology and Hepatology, Osaka University Graduate School of Medicine, 2-2, Yamada-oka, Suita, Osaka 565-0871, Japan; and ⁷Department of Disease Glycomics, Research Institute for Microbial Diseases, Osaka University, Center for Advanced Science & Innovation, 2-1, Yamada-oka Suita, Osaka 565-0871, Japan

Received on April 27, 2007; revised on August 09, 2007; accepted on August 31, 2007

Changes in the levels of fucosylation regulate the biological phenotype of cancer cells and a specific fucosylation, such as fucosylated α -fetoprotein (AFP-L3) has been clinically used as a tumor marker for hepatocellular carcinoma (HCC). However, detailed molecular mechanisms that explain the increased fucosylation in HCC remain unknown despite 10 years of study by these researchers. Fucosylation is regulated by complicated mechanisms that involve several factors: fucosyltransferases, GDP-fucose transporter (GDP-Fuc Tr), and synthetic enzymes of GDP-fucose, such as GDP-mannose 4, 6-dehydratase (GMD), GDP-4-keto-6-deoxy-mannose-3, 5-epimerase-4-reductase (FX), and GDP-fucose pyrophosphorylase. In this study, the expression of fucosylation-related genes in HCC tissues was studied and it was found that GDP-Fuc Tr is a key factor for increases in fucosylation. A real-time reverse transcription polymerase chain reaction (RT-PCR) analysis showed significant increases in GDP-Fuc Tr and FX expression in HCC, and levels of the GMD protein were upregulated by posttranslational modification in HCC tissues. In vitro cell experiments showed that the level of GDP-Fuc Tr was the most significantly correlated with the level of cellular fucosylation and the overexpression of GDP-Fuc Tr dramatically increased fucosylation in Hep3B cells. The importance of GDP-Fuc Tr in the increase of fucosylation was also confirmed with immunohistochemical analyses. These findings suggest that the upregulation of GDP-Fuc Tr plays a pivotal role in increased fucosylation in HCC and represents an attractive target for new treatments and diagnosis for HCC.

Keywords: AFP-L3/fucose/GDP-fucose/GDP-fucose transporter/hepatocellular carcinoma

Introduction

Oligosaccharides are one of the most important factors in the posttranslational modification of proteins. It is a well-known fact that oligosaccharide structures are changed during malignant transformations (Hakomori et al. 1989). Therefore, oligosaccharides have been used as bio-markers for various types of tumors and have the potential to become targets for effective treatment. While alpha-fetoprotein (AFP) has been clinically used as a tumor marker for hepatocellular carcinoma (HCC) (Alpert et al. 1968), its levels are also increased in chronic liver diseases, such as chronic hepatitis (CH) and liver cirrhosis (LC). Therefore, it is difficult to make a diagnosis of HCC that is differential from chronic liver diseases based on low or medial elevations of AFP – making it of questionable value as a tumor marker (Chen et al. 1977; Ebara et al. 1986). Under these circumstances, fucosylated AFP (AFP-L3 fraction) is more effective for the specific diagnosis of HCC because it increases in patients with HCC, but not CH and LC (Aoyagi et al. 1985; Taketa et al. 1993). The measurement of fucosylated AFP for the diagnosis of HCC has been clinically applied in Japan since 1996 and was approved by the Food and Drug Administration (FDA) in the United States in 2005.

This research group previously succeeded in the purification and cDNA cloning of α 1-6 fucosyltransferase (α 1-6 FucT), which catalyzes the transfer of a fucose residue to the reducing end GlcNAc in complex *N*-glycans via an α 1-6 linkage (Uozumi et al. 1996; Yanagidani et al. 1997). α 1-6 FucT is responsible for the fucosylation of AFP. The expression level of α 1-6 FucT mRNA was found to be increased in hepatic tumor lesions, but not in adjacent lesions in a hepatocarcinogenic model rat, the Long-Evans with cinnamon-like coat color rat (LEC rat) (Noda et al. 1998). However, in human liver, α 1-6 FucT was increased in both HCC tissues and the adjacent tissues, which exhibited CH or LC (Noda et al. 1998). These results indicate that the fucosylation of AFP in HCC is regulated not only by the direct upregulation of α 1-6 FucT, but also by other mechanisms.

Guanosine 5'-diphosphate (GDP)-fucose is a donor substrate common to all fucosyltransferases, including α 1-6 FucT, and its level is increased in HCC (Noda et al. 2003). GDP-fucose is synthesized in the cytosol via two pathways, namely the salvage pathway and the de novo pathway (Figure 1). The salvage pathway synthesizes GDP-fucose from free L-fucose derived from extracellular or lysosomal sources via two steps: catalyzation by L-fucokinase (Park et al. 1998) and GDP-fucose pyrophosphorylase (Pastuszak et al. 1998). The de novo pathway transforms GDP-mannose into GDP-fucose via three steps: catalyzation by GDP-mannose 4, 6-dehydratase (GMD) (Ohshima et al. 1998;

¹To whom correspondence should be addressed: Tel and Fax: +81-6-6879-2590; e-mail: emiyoshi@sahs.med.osaka-u.ac.jp

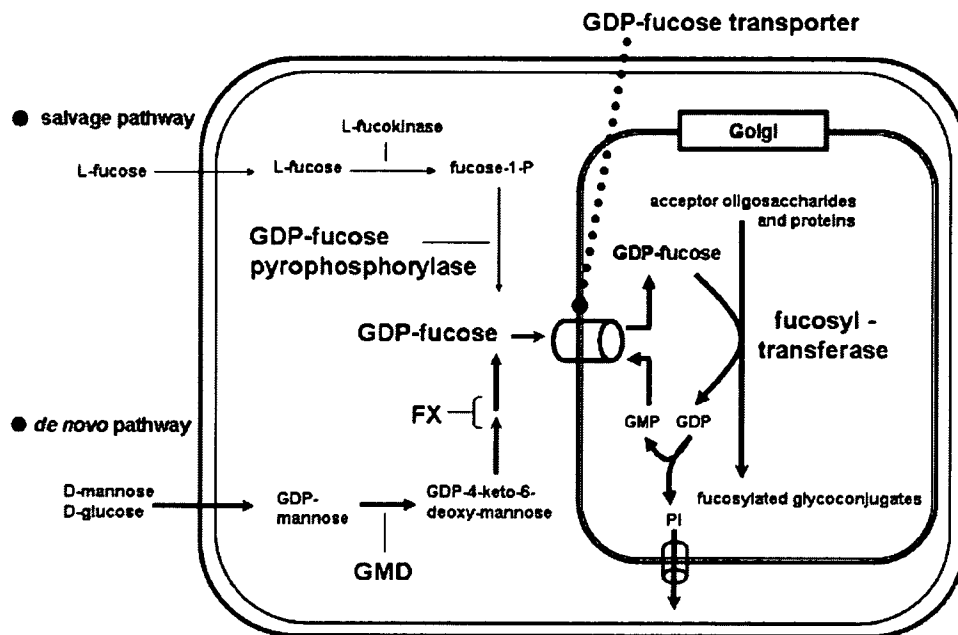


Fig. 1. Fucose metabolism. Free L-fucose is converted to GDP-fucose by the salvage pathway. GDP-fucose is also synthesized by the de novo pathway via three reactions catalyzed by GMD and FX. GDP-fucose is subsequently transported from the cytosol to the Golgi lumen by GDP-Fuc Tr and transferred to acceptor oligosaccharides and proteins. GDP, the other reaction product, is converted by a luminal nucleotide diphosphatase to guanosine 5'-monophosphate (GMP) and inorganic phosphate (Pi). The former is exported to the cytosol through an antiport system that is coupled with the transport of GDP-fucose, whereas the latter is postulated to leave the Golgi lumen via the Golgi anion channel, GOLAC (Nordeen et al. 2000; Hirschberg et al. 2001).

Sullivan et al. 1998) and GDP-4-keto-6-deoxy-mannose-3, 5-epimerase-4-reductase, also known as FX (Tonetti et al. 1996). The salvage pathway contributes to only about 10% of the cellular pool of GDP-fucose. Thus, the de novo pathway mainly produces cellular GDP-fucose. This research group previously established a unique method for the determination of GDP-fucose levels in cytosolic fractions using isocratic reverse phase high performance liquid chromatography (HPLC) (Noda et al. 2002). Using this method and Northern blot analysis, we found that both the levels of GDP-fucose and the expression of FX mRNA were significantly increased in HCC tissue compared with adjacent tissue or the tissue of normal livers (Noda et al. 2003). However, the level of cellular fucosylation did not always correlate with these parameters.

While fucosylation catalyzed by fucosyltransferases takes place in the Golgi apparatus, GDP-fucose is synthesized in the cytosol. Therefore, GDP-fucose must be transported by a GDP-fucose transporter (GDP-Fuc Tr), a transmembrane protein in the Golgi, to serve as a substrate of fucosyltransferases. Kumamoto et al. reported that the expression level of UDP-galactose transporter mRNA was significantly increased in colon cancer tissues compared with nonmalignant mucosal tissues, resulting in a possible enhancement of metastatic capacity (Kumamoto et al. 2001). This study showed that the UDP-galactose transporter could regulate the influx of UDP-galactose from the cytosol into the Golgi lumen, leading to the modulation of oligosaccharide structures via reactions of galactosyltransferases. These facts suggest that a transporter as well as synthetic enzymes of GDP-fucose are likely to play pivotal roles in the regulation of fucosylation.

Zipin et al. proposed that GDP-fucose controls the metastatic capacity of colorectal cancer and could become a target for

metastatic prevention (Zipin et al. 2004). In this study, the expression levels of genes responsible for the transport and synthesis of GDP-fucose in HCC tissues were investigated, and the main contributors to the fucosylation of HCC were determined by in vitro experiments. Furthermore, these results were confirmed with an immunohistochemical study using 59 cases of HCC tissue. GDP-Fuc Tr was found to play the most critical role in the fucosylation of HCC among many factors, including fucosyltransferases and GDP-fucose synthetic enzymes.

Results

Levels of fucosylation-related genes among normal livers, HCC tissues, and adjacent tissues

The expression of GDP-Fuc Tr, FX, GMD, GDP-fucose pyrophosphorylase and α 1-6 FucT mRNA was investigated by real-time RT-PCR analysis using 13 human HCC tissues and two normal liver tissues (Figure 2). The expression of GDP-Fuc Tr and FX were significantly increased in HCC compared with chronic liver disease (CH and LC) or normal liver (HCC versus chronic liver disease, $P = 0.035$ and 0.019 , HCC versus normal liver, $P = 0.022$ and <0.01 , respectively, by one-way ANOVA followed by the protected least significant differences (PLSD) test). In contrast, no significant differences were observed in the expression of GMD, GDP-fucose pyrophosphorylase, and α 1-6 FucT among HCC, chronic liver disease, and normal liver. In individual cases, GDP-Fuc Tr and FX were also significantly increased in HCC compared with the adjacent tissue ($P = 0.036$ and <0.01 , respectively, by the paired t test) (Supplementary data, Figure 1). None of the other genes showed significant

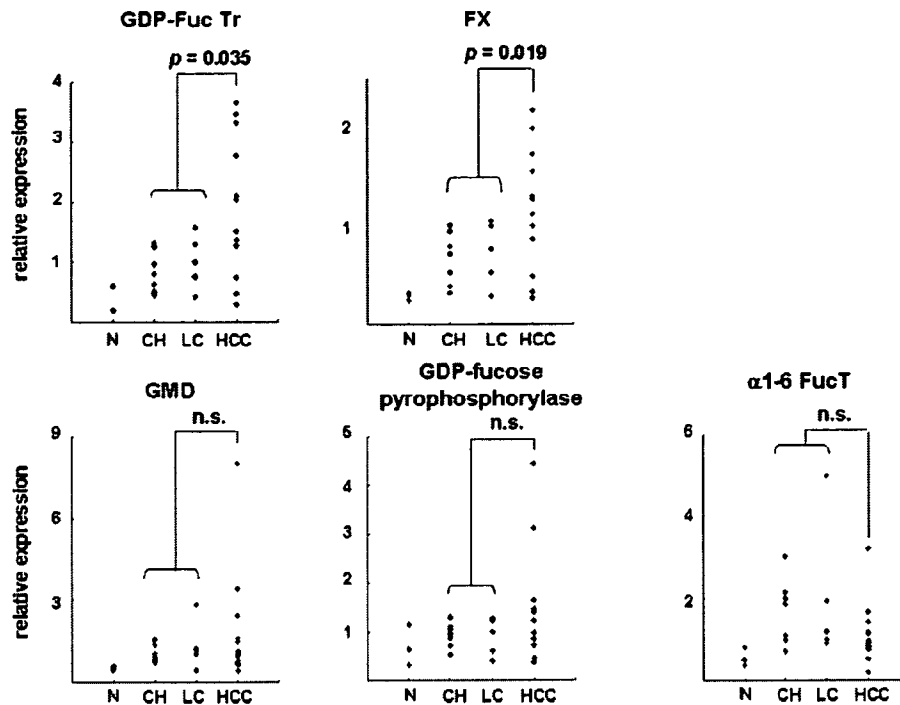


Fig. 2. Real-time RT-PCR analyses for the expression of GDP-Fuc Tr, FX, GMD, GDP-fucose pyrophosphorylase, and α 1-6 FucT mRNA. The expression levels of GDP-Fuc Tr, FX, GMD, GDP-fucose pyrophosphorylase, and α 1-6 FucT mRNA were compared among normal liver ($n = 3$), chronic liver disease (CH [$n = 7$], LC [$n = 5$]), and HCC ($n = 13$). In GDP-Fuc Tr mRNA, HCC versus chronic liver disease, $P = 0.035$; HCC versus normal liver, $P = 0.022$. In FX mRNA, HCC versus chronic liver disease, $P = 0.019$; HCC versus normal liver, $P < 0.01$. In GMD, GDP-fucose pyrophosphorylase, and α 1-6 FucT mRNA, HCC versus chronic liver disease or normal liver, was not significant. Statistical analysis was performed by one-way ANOVA followed by the PLSD test. n , number of specimens examined. n.s., not significant.

differences. In all the genes investigated, no significant difference was observed between CH and LC, suggesting that the up-regulation of fucosylation-related genes is not associated with the progression of chronic liver diseases. The expression of fucosylation-related genes, except for GDP-fucose pyrophosphorylase, in chronic liver diseases was increased compared with normal livers, but the increases were not significant due to the small number of normal liver samples (3 patients). A study using a larger number of samples would allow us to detect statistically significant differences between chronic liver disease and normal liver. These results indicate that GDP-Fuc Tr is increased in HCC compared with chronic liver disease, and might be involved in the increased fucosylation in HCC.

Western blot analysis of GMD

GMD is one of the most important rate limiting enzymes in the de novo pathway of GDP-fucose synthesis. While the results of real-time RT-PCR using human HCC tissues did not show a significant increase in the level of GMD mRNA, we investigated the expression level of the GMD protein by western blot analysis. As shown in Figure 3A, the expression level of the GMD protein was markedly increased in HCC tissues. Moreover, the expression level of GMD protein in HCC was increased compared with chronic liver disease and normal liver, as analyzed densitometrically (HCC versus chronic liver disease, $P < 0.01$, HCC versus normal liver, $P = 0.014$, by one-way ANOVA followed by the PLSD test) (Figure 3B). The protein and mRNA levels of GMD were not correlated, particularly in

cases of a low expression of its mRNA, suggesting that unknown posttranslational regulations are responsible for the increase of GMD protein in HCC (Figure 3C). These results indicate that the increased level of GDP-fucose in HCC is due to the up-regulation of the expression levels of FX and GMD, followed by activation of the de novo pathway.

Fucosylation level of hepatoma cells in terms of GDP-fucose transporter, FX, and GMD

To determine which factors are important for the increased fucosylation among GDP-Fuc Tr, FX, and GMD, we compared the expression levels of these molecules with the fucosylation levels in five hepatoma cells (Hep3B, HepG2, HLE, HLF, and Huh7). We first determined the expression levels of GDP-Fuc Tr, FX, and GMD in hepatoma cells by either real-time RT-PCR analysis or western blot analysis (Figure 4A and B). The expression level of the GDP-Fuc Tr was higher in HepG2 and Huh7 cells, but lower in Hep3B, HLE, and HLF cells. The expression levels of FX and GMD were higher in Hep3B, HepG2, and Huh7 cells, but lower in HLE and HLF cells. We subsequently performed a lectin blot analysis with *Aleuria aurantia lectin* (AAL) to investigate the fucosylation level in each of the hepatoma cells. The AAL lectin recognizes fucosylated oligosaccharides. In HepG2 and Huh7 cells, numerous proteins were strongly fucosylated, but in Hep3B, HLE, and HLF cells, the fucosylation was weak (Figure 4C). These results suggest that the up-regulation of GDP-Fuc Tr is much more important for increases in fucosylation.

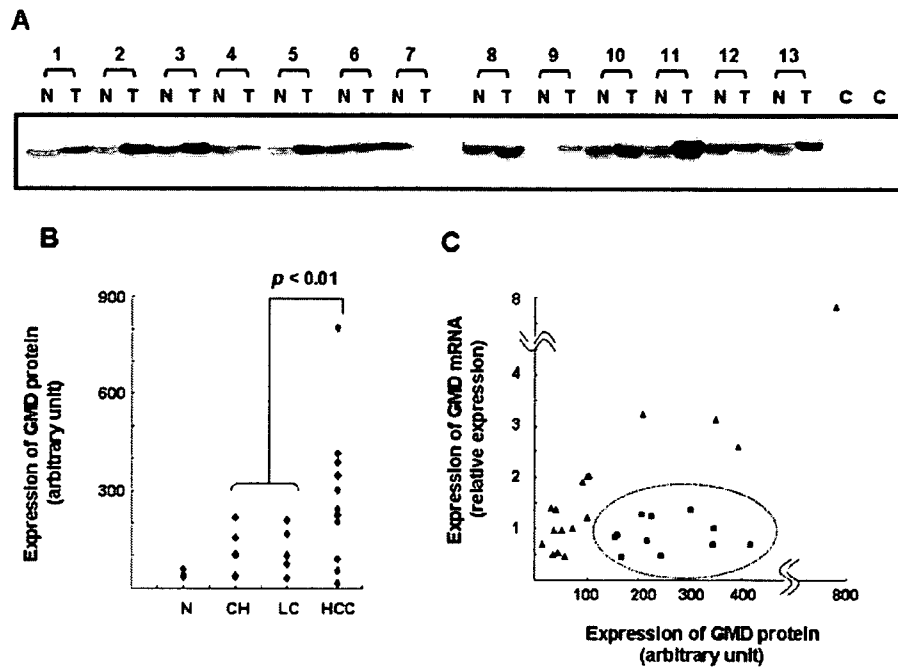


Fig. 3. Western blot analysis of the expression of GMD. (A) Cytosolic proteins extracted from HCC tissue, adjacent tissue, and normal liver tissue were electrophoresed on 10% acrylamide gels. Then a western blot analysis of GMD, using an anti-GMD polyclonal antibody, was performed. Detailed procedures are described in "Materials and methods." T, HCC tissue; N, adjacent tissue; C, control. (B) The expression of GMD was compared among HCC, chronic liver disease, and normal liver. HCC versus chronic liver disease, $P < 0.01$; HCC versus normal liver, $P = 0.014$, by one-way ANOVA followed by the PLSD test. (C) Comparison of GMD mRNAs and proteins. Relative levels of GMD mRNA detected by real-time RT-PCR and relative levels of its protein measured by western blot are compared. The group described by the square dot in the dotted circle showed no correlation between protein and mRNA of GMD.

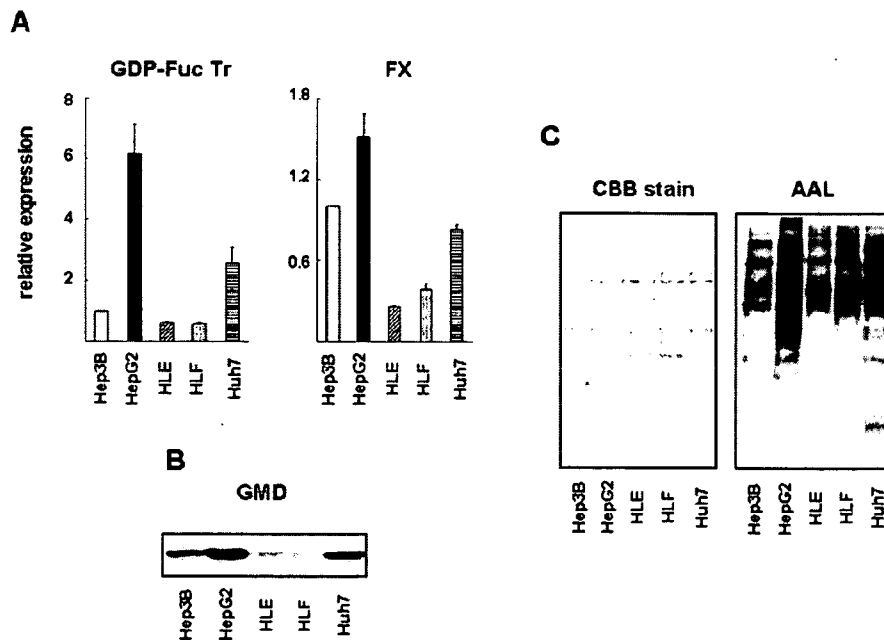


Fig. 4. Analysis of the expression level of GDP-Fuc Tr, FX, and GMD and the fucosylation level in hepatoma cells. (A) Expression levels of GDP-Fuc Tr and FX mRNA were demonstrated by real-time RT-PCR analysis in hepatoma cells, Hep3B, HepG2, HLE, HLF, and Huh7. The results are represented as relative units compared with Hep3B and the means of three independent experiments (bars), SD. (B) Expression level of the GMD protein was evaluated by western blot analysis. (C) Cellular fucosylation levels were evaluated in hepatoma cells. Detailed procedures are described in "Materials and methods." Coomassie Brilliant Blue (CBB) staining indicated that equal amounts of protein were loaded in each lane.